Supplement of:

Development of a thermal desorption-gas chromatography-mass spectrometry method for the analysis of monoterpenoids, sesquiterpenoids and diterpenoids

A. Helin[1], H. Hakola[1] and H. Hellén[1]

[1]Atmospheric Composition Research, Finnish Meteorological Institute, Helsinki, FI-00101, Finland

*Corresponding author: aku.helin@fmi.fi

Summary of number of pages, figures and tables:

Number of Pages: 36

Number of Tables: 5

Number of Figures: 23

Contents

Table S1. List of chemicals used in this study.

Compound	CAS Number	Purity	Supplier
α-pinene	7785-70-8	analytical standard	Sigma-Aldrich (St.Louis, MO, USA)
camphene	79-92-5	95 %	Sigma-Aldrich (Steinheim, Germany)
β-pinene	19902-08-0	analytical standard	Sigma-Aldrich (St.Louis, MO, USA)
3-carene	498-15-7	analytical standard	Sigma-Aldrich (St.Louis, MO, USA)
p-cymene	99-87-6	analytical standard	Sigma-Aldrich (St.Louis, MO, USA)
limonene	5989-54-8	≥99.0 %	Sigma-Aldrich (Buchs, Switzerland)
1,8-cineol	470-82-6	99 %	Sigma-Aldrich (Gillingham, Dorset, UK)
terpinolene	586-62-9	~95 %	Fluka Chemie AG (Buchs, Switzerland)
linalool	78-70-6	97 %	Sigma-Aldrich (St.Louis, MO, USA)
4-acetyl-1-methylcyclohexene (4-AMCH)	6090-09-1	98 %	Sigma-Aldrich (Milwaukee, WI, USA)
nopinone	38651-65-9	98 %	Sigma-Aldrich (St.Louis, MO, USA)
bornylacetate	5655-61-8	97 %	Sigma-Aldrich (Milwaukee, WI, USA)
longicyclene	1137-12-8	≥95 %	Sigma-Aldrich (St.Louis, MO, USA)
isolongifolene	1135-66-6	≥98 %	Sigma-Aldrich (St.Louis, MO, USA)
β-caryophyllene	87-44-5	≥98.5 %	Sigma-Aldrich (St.Louis, MO, USA)
β-farnesene	18794-84-8	≥90 %	Sigma-Aldrich (St.Louis, MO, USA)
α-humulene	6753-98-6	≥96.0 %	Sigma-Aldrich (St.Louis, MO, USA)
caryophyllene oxide	1139-30-6	≥99.0 %	Sigma-Aldrich (St.Louis, MO, USA)
cembrene	1898-13-1	95 %	Combi-Blocks (San Diego, CA, USA)
ent-kaurene	562-28-7	90 %	BOC Sciences (info@bocsci.com)
3-methylene-5-α-androstane (3-MA)	Not assigned	crude	Sigma-Aldrich (St.Louis, MO, USA)
methanol	67-56-1	≥99.9 %	VWR Chemicals (Gliwice, Poland)
ultrapure water	-	-	Milli-Q Gradient (Molsheim, France)
C_8-C_{40} alkanes calibration standard (in dichloromethane)	-	-	Sigma-Aldrich (St.Louis, MO, USA)

Table S2. Both TD-GC-MS's instrumental parameters and analysis conditions presented.

Equipment/Parameter	TD-GC-MS 1	TD-GC-MS 2
Thermal desorption unit	TurboMatrix 350 (PerkinElmer Inc., Waltham, MA, USA)	TurboMatrix 650 (PerkinElmer Inc., Waltham, MA, USA)
Cold trap	Tenax TA/Carboback B (PerkinElmer Inc., Waltham, MA, USA)	Tenax TA (PerkinElmer Inc., Waltham, MA, USA)
Pre-purge time [sorbent tube purging]	1 min (He flow rate 50 mL/min)	5 min (He flow rate 50 mL/min)
Primary desorption [sorbent tube desorption]	5 min at 300 °C (desorption flow rate 50 mL/min, no split flow applied)	5 min at 300 °C (desorption flow rate 50 mL/min, no split flow applied)
Secondary desorption [cold trap desorption]	Initial temperature 20 °C, then heated to 300 °C for 1 min. (desorption flow rate 10 mL/min, outlet split)	Initial temperature 20 °C, then heated to 300 °C for 5 min (desorption flow rate 30 mL/min, outlet split)
Heated valve temperature	220 °C	220 °C
Heated transfer line [between TD and GC]	deactivated fused silica (ca. 1 m x 0.25 (i.d.)), Agilent Technologies, Palo Alto, USA) heated to 200 °C	deactivated fused silica (ca. 1 m x 0.25 (i.d.)), Agilent Technologies, Palo Alto, USA) heated to 200 °C
Gas chromatograph	Clarus 680 (PerkinElmer Inc., Waltham, MA, USA)	Clarus 600 (PerkinElmer Inc., Waltham, MA, USA)
Column	Elite-5 MS (60 m x 0.25 mm (i.d.), 0.25 um film thickness, PerkinElmer Inc., Waltham, MA, USA)	DB-5MS (50 m x 0.25 mm (i.d.), 0.25 um film thickness, Agilent Technologies, Palo Alto, USA)
Temperature program	60 °C (2 min) --> 300 °C at 8 °C /min --> 300 °C (15 min)	60 °C (2 min) --> 300 °C at 8 °C /min --> 300 °C (3 min)
Flow rate	1 mL/min (constant flow mode)	1 mL/min (constant flow mode)
Carrier gas	Helium (≥ 99.9996 %, AGA, Espoo, Finland)	Helium (≥ 99.9996 %, AGA, Espoo, Finland)
Interface temperature	220 °C	220 °C
Mass spectrometer	Clarus SQ 8 T (PerkinElmer Inc., Waltham, MA, USA)	Clarus 600 T (PerkinElmer Inc., Waltham, MA, USA)
Mass analyzer	quadrupole	quadrupole
Ion source temperature	150 °C	150 °C
Electron ionization	70 eV	70 eV
Scan range	m/z 50-350	m/z 50-350
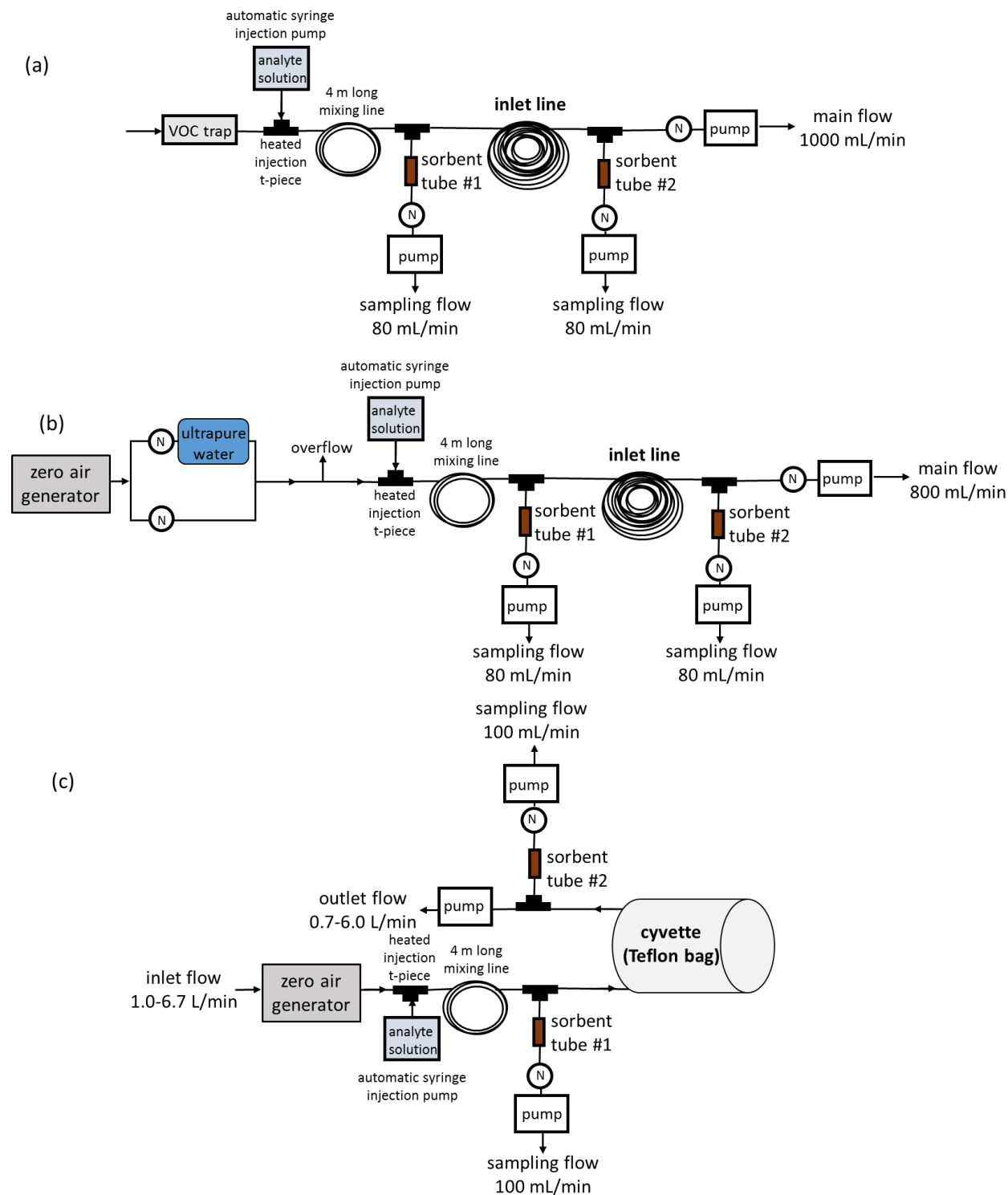
Figure S1. Illustration of the experimental setups used in the inlet line sampling **(a-b)** and cuvette **(c)** recovery experiments. **(a)** Experiments performed at room temperature and relative humidity (RH). **(b)** Experiments performed at room temperature at different RH levels. In both (a) and (b), the analyte solution was injected at a flow rate of 15 µL/h and the sorbent sampling time was 20 min. In **(c)**, the injection flow rate was between 20-105 µL/h and the sampling time was 30 min. In all experiments, the injection t-piece was heated to 60±5 °C.
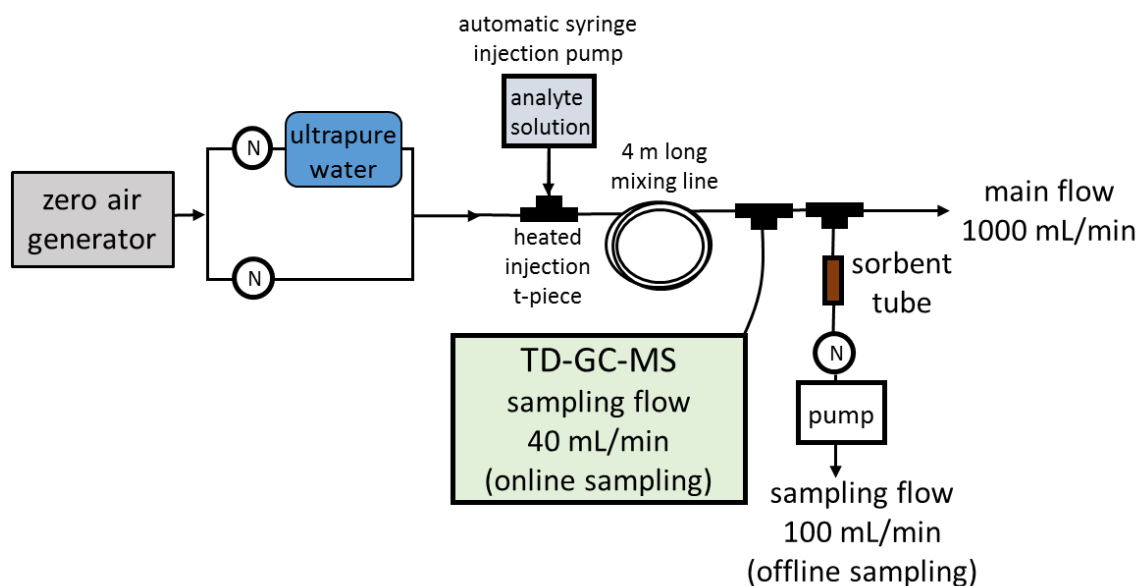
Figure S2. Schematic illustration of the experimental setup used for the comparison of online and offline mode TD-GC-MS sampling and analysis. The analyte solution was injected at a flow rate of 60 µL/h, the injection t-piece was heated to 60±5 °C and the mixing line was a 4 m long Teflon tubing (i.d. 1/8 in.). In the online TD-GC-MS mode, the sampling line length from the t-piece to the instrument inlet port was approximately 2 m Teflon tubing (i.d. 1/16 in.). Sampling time with both sampling modes was 30 min.
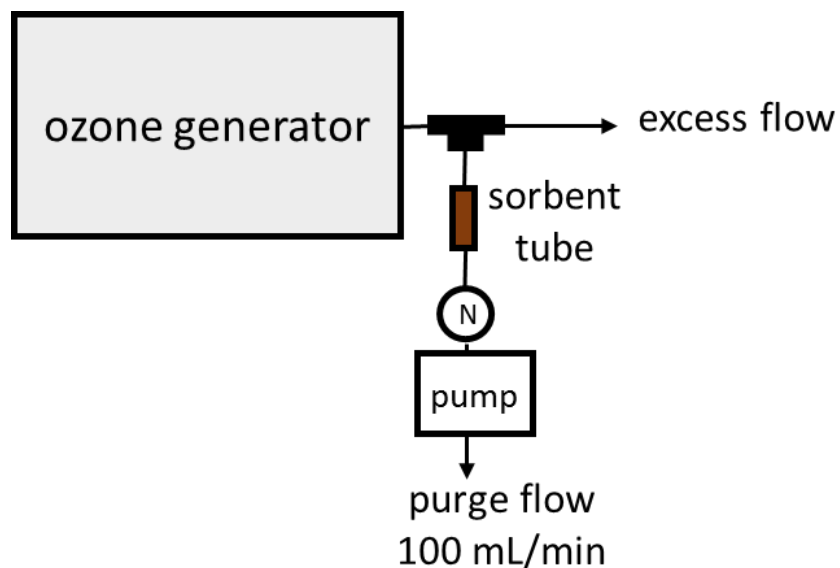
Figure S3. Illustration of the experimental setup used for studying of the compound stability in sorbent tube upon ozone exposure. The ozone generator was used to produce either $O_3=0$ ppb or $O_3=40$ ppb concentrations. The analyte amounts in sorbent tube were in the range of 40-200 ng. The purge volume was between 0-24 L.
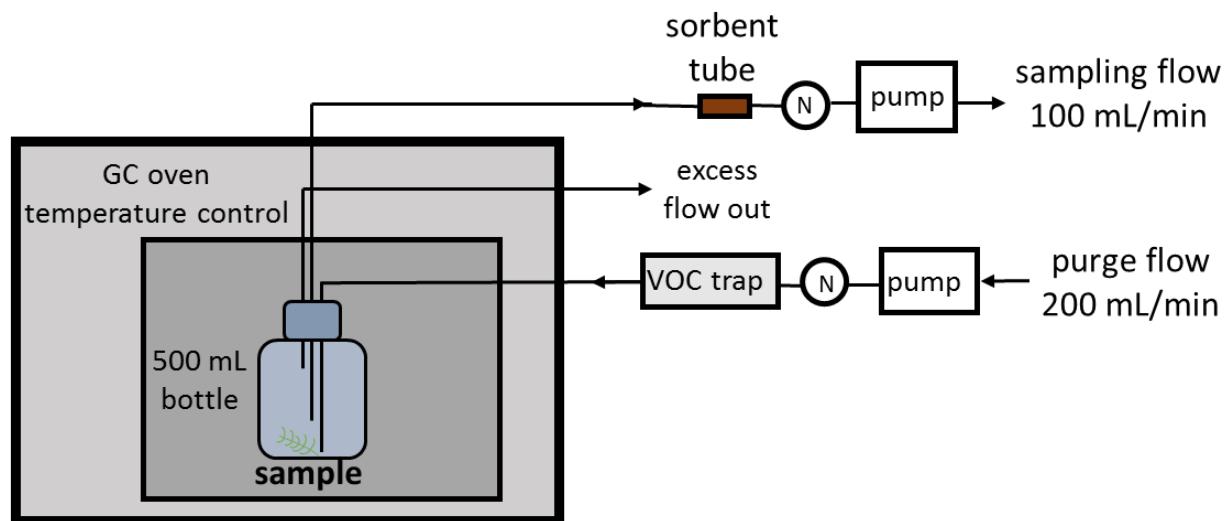
Figure S4. Illustration of the experimental setup used for the purge-and-trap type of headspace extraction of the pine needles and spruce twigs. The samples were placed inside a 500 mL glass bottle, purified air (active carbon cartridge for VOC trapping) was passed into the bottle and the sorbent tube sample was taken from one outlet line (the other outlet line was exhaust for excess flow). The glass bottle was heated in 5-10 °C steps from room temperature to 70 °C.
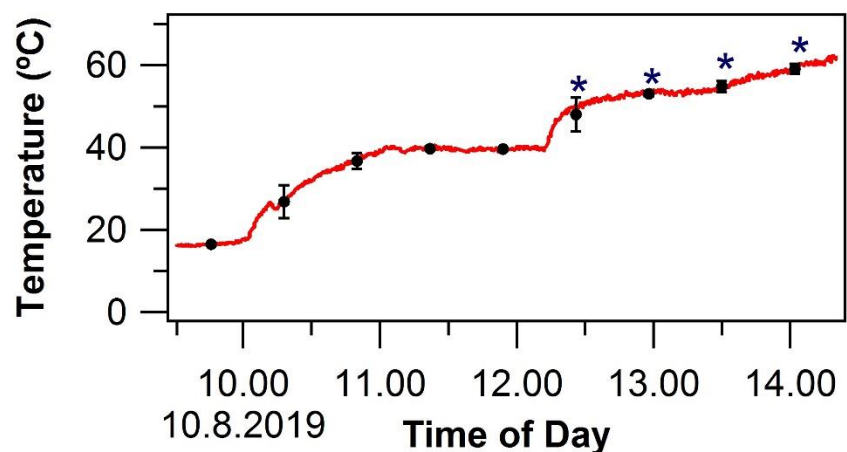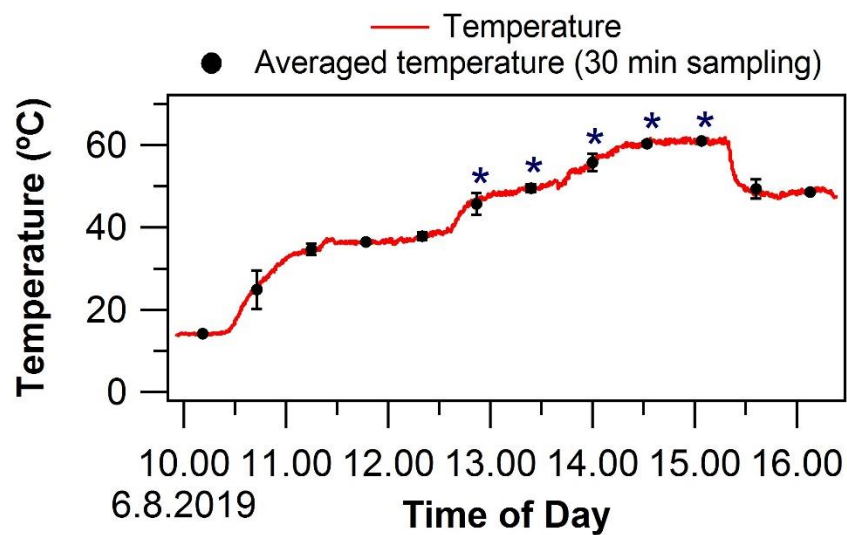
Figure S5. Cuvette inside temperature during the heating cycle on the different sampling dates of branch enclosure emission experiments. The average (± standard deviation) temperature corresponding to the 30 min offline sorbent tube sampling times are plotted on mid-point of sampling. The asterisk points indicate times during which the cuvette was covered with aluminium foil.
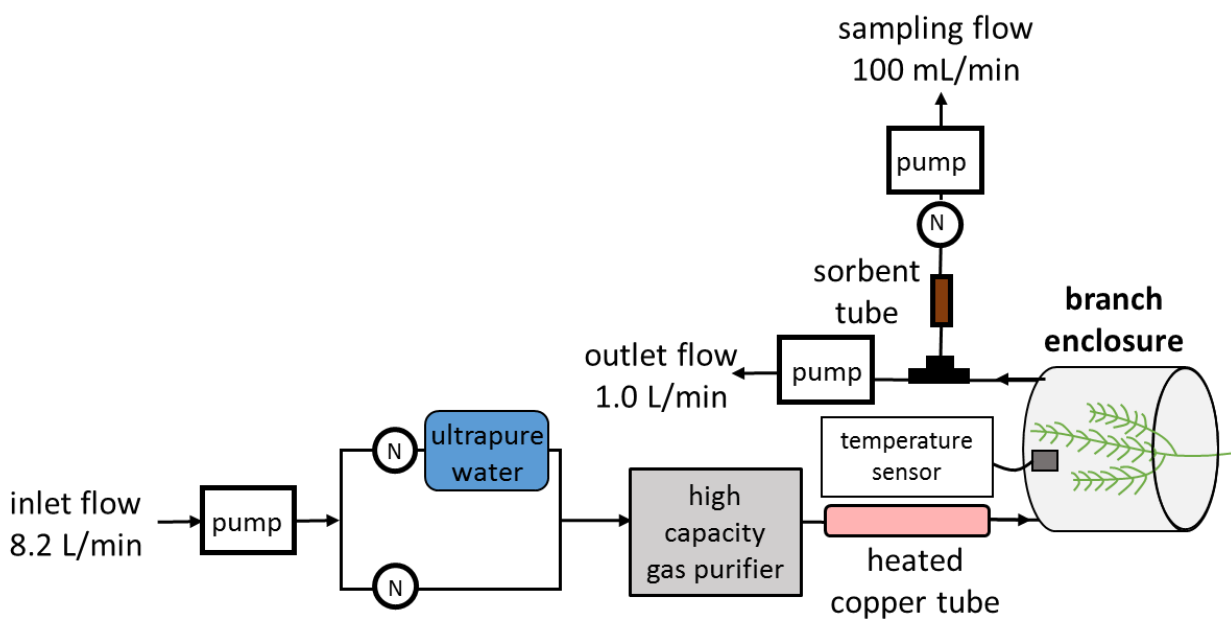
Figure S6. Schematic illustration of the setup used for branch enclosure emission measurements. The schematic presented here corresponds to the setup used on 6th of August, 2019 when the offline sorbent tube sampling was performed from a bypass line. On 10th of August, 2019 the offline sorbent tube sampling (at 100 mL/min for 30 min) was performed directly from the cuvette outlet.
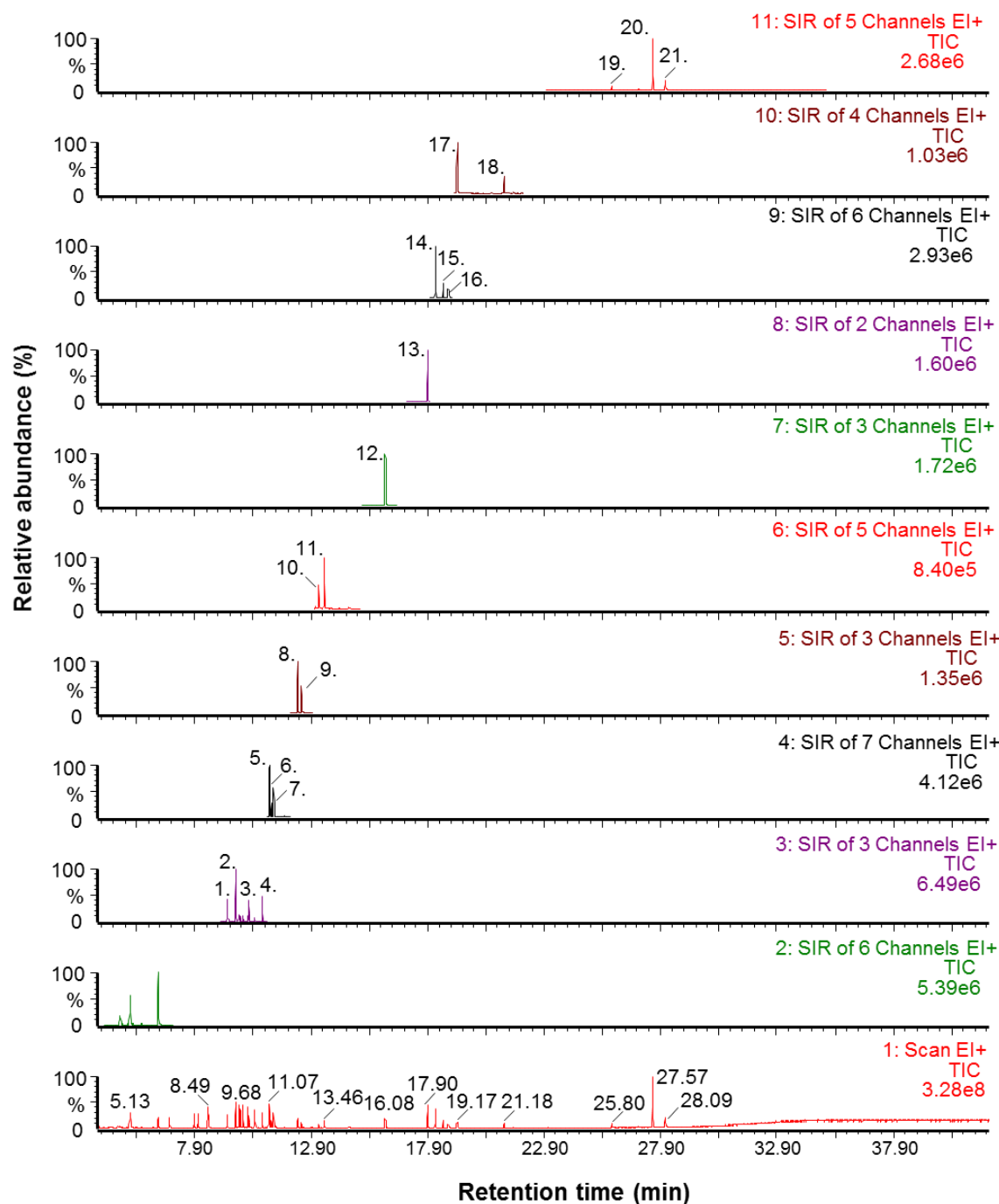
Figure S7. TD-GC-MS total ion chromatogram (TIC, bottom row 1) and selected ion recording (SIR, 2-11) chromatograms of a standard solution analysis (c=10-50 ng in sorbent tube). Analysis conditions are presented in Table S2 (TD-GC-MS1). Peak identification: 1. α-pinene, 2. camphene, 3. β-pinene, 4. 3-carene, 5. *p*-cymene, 6. limonene, 7. 1,8-cineol, 8. terpinolene, 9. linalool, 10. 4-AMCH, 11. nopinone, 12. bornylacetate, 13. longicyclene, 14. isolongifolene, 15. β-caryophyllene, 16. β-farnesene, 17. α-humulene, 18. caryophyllene oxide, 19. cembrene, 20. ent-kaurene and 21. 3-MA. For abbreviations see main text Table 1 or Table S1.
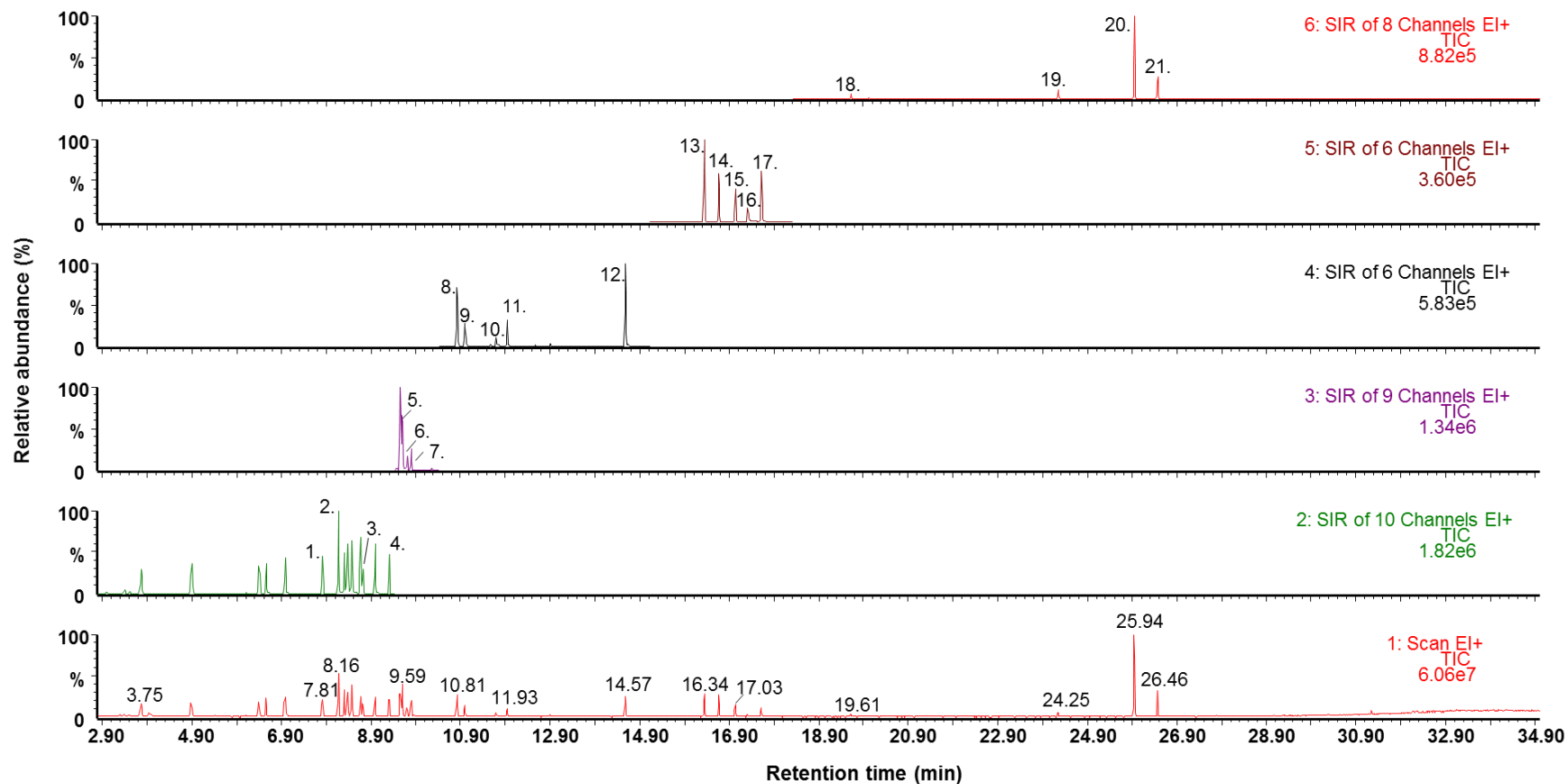
Figure S8. TD-GC-MS total ion chromatogram (TIC, bottom row 1) and selected ion recording (SIR, 2-6) chromatograms of a standard solution analysis (c=10-50 ng in sorbent tube). Analysis conditions are presented in Table S2 (TD-GC-MS2). Peak identification: 1. α-pinene, 2. camphene, 3. β-pinene, 4. 3-carene, 5. *p*-cymene, 6. limonene, 7. 1,8-cineol, 8. terpinolene, 9. linalool, 10. 4-AMCH, 11. nopinone, 12. bornylacetate, 13. longicyclene, 14. isolongifolene, 15. β-caryophyllene, 16. β-farnesene, 17. α-humulene, 18. caryophyllene oxide, 19. cembrene, 20. ent-kaurene and 21. 3-MA. For abbreviations see main text Table 1 or Table S1.
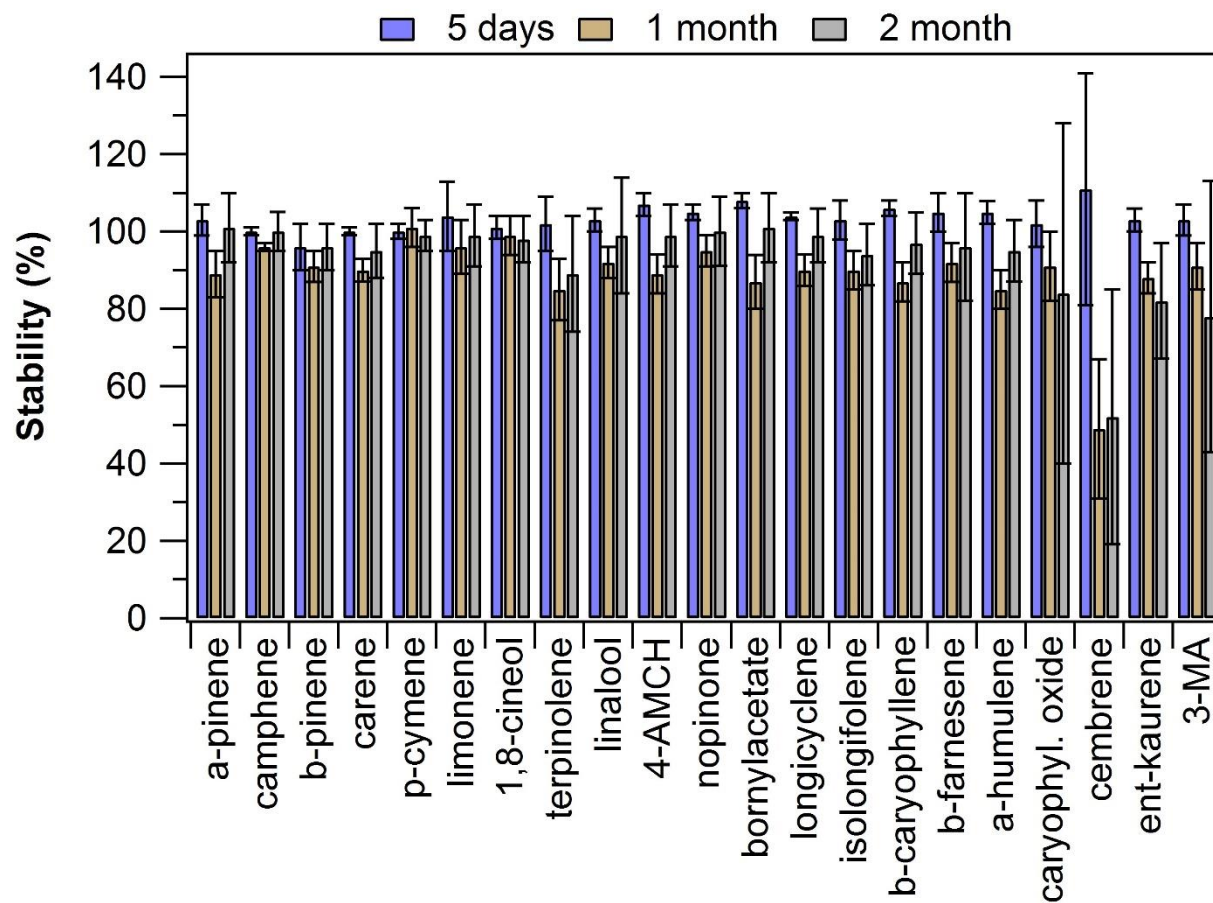
Figure S9. Stability of the analytes in sorbent tube (c=40-200 ng) during storage (5 days, 32-33 days and 62 days) in the dark at 4°C. The error bars represent reproducibility (*n*=2-6).
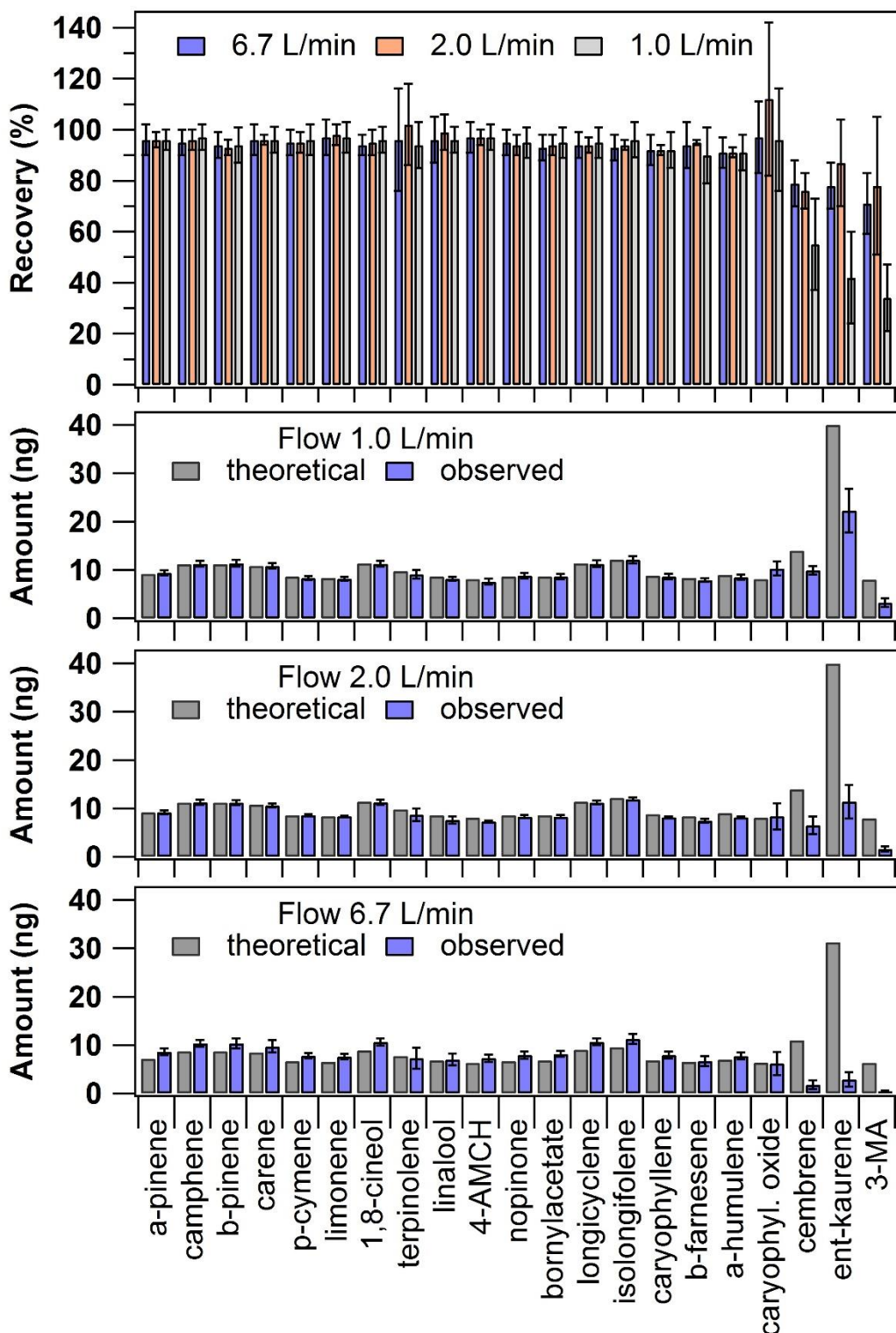
Figure S10. Cuvette recovery results and the absolute amount detected in the first sampling sorbent tube presented according to the different inlet flow rates used. The theoretical expected amount was calculated based on the used experimental conditions. The error bars represent reproducibility (*n*=3-9).

TEXT S1. Comparison between online and offline TD-GC-MS sampling

S1.1 Overview of comparison parameters and conditions

As outlined in the main text Section 2.3.4, online sampling mode was compared to offline sampling mode with TD-GC-MS1. The experiments were done as shown in the schematic setup shown in Fig. S2. The sampling flow rate was 40 mL/min for 30 min in online mode sampling (total volume 1.2 L). The online sampling was performed via an empty stainless-steel tube directly into the Tenax TA/Carbopack cold trap (Fig. S11). In the offline sorbent tube sampling, the flow rate was 100 mL/min for 30 min (sampling volume 3.0 L). The online and offline mode sampling times were harmonized. The analyte concentrations were typically in the level of 9.3-13.2 µg/m^3 for MTs, 8.4-13.8 µg/m^3 for SQTs, 1.7-11.4 µg/m^3 for DTs and 8.8-9.9 µg/m^3 for other VOCs. The analytes were always injected as a mixture of all compounds.
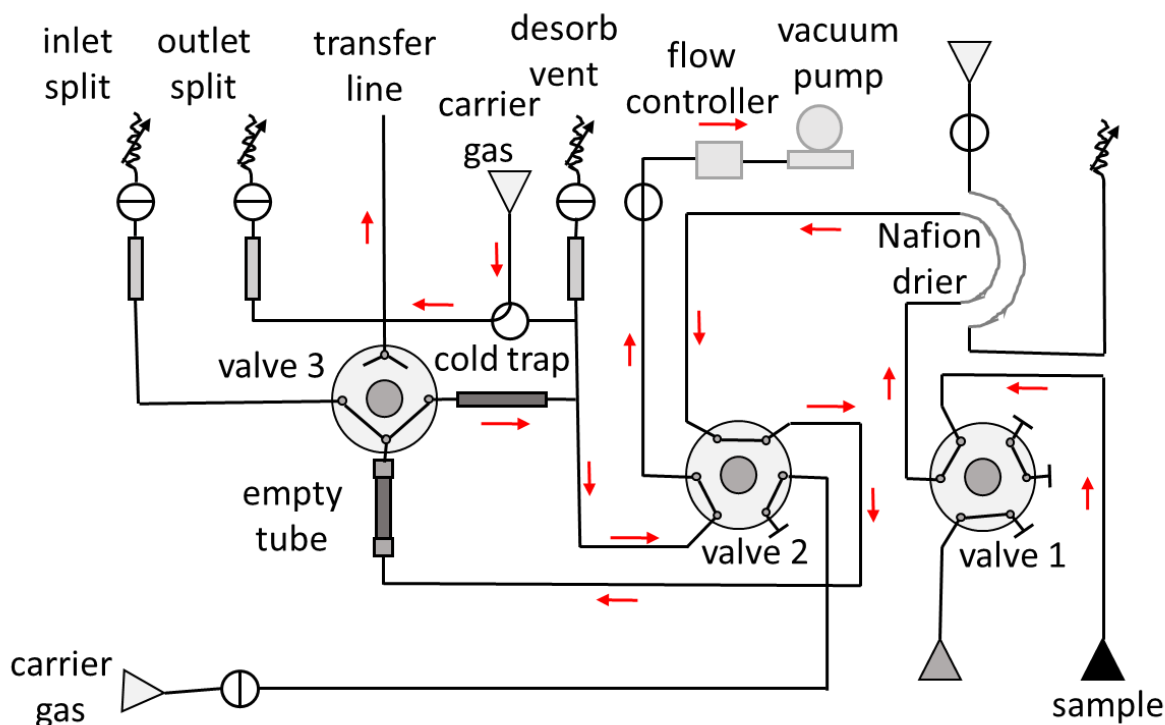
Figure S11. Schematic diagram of the conventional online sampling mode in the TD (adapted from instrument user's guide). The red arrows indicate the online sampling mode flow directions. In the TD unit used in this study, the Nafion drier was replaced with a ca. 10 cm long Teflon tubing (i.d. 1/16 in.).

The TD-GC-MS analysis conditions were otherwise exactly the same with both sampling modes (see Table S2), with the exception that in the online mode there was no primary desorption step. In online sampling mode, the sample is drawn in through an empty tube held at room temperature and directly focused onto the cold trap. Thus, there is theoretically no need for primary desorption. In online sampling mode, the instrument software allows only an option to control the secondary desorption.

The different sampling mode results were compared to each other based on recoveries as shown in equation:

$$\text{Recovery} = \frac{\text{analyte concentration in online mode (µg/m}^3)}{\text{analyte concentration in offline mode (µg/m}^3)} * 100\%$$

S1.2 Initial trials and problem identification

It was observed that some of the analytes were lost in the online sampling mode. In the TD unit, an empty sorbent tube was used in the online mode to connect the online sampling box to the main TD (see Fig. S11). This empty tube has a high surface area compared to the other TD parts in the sample path and therefore is a probable source of poor recoveries. To test the losses into the empty stainless-steel tube used in online sampling, the empty tube was heated after the sampling to 300 °C and compounds desorbed were analyzed. In this re-analysis of the empty tube, multiple different compounds could be detected in surprisingly high amounts. For example, β-farnesene was observed in the empty tube in such a high amounts, that it would explain approximately 44 % of the amount lost during online sampling. Ent-kaurene and cembrene were observed in the empty tube in amounts that would explain roughly 2 % and 12 % of the lost fraction, respectively. For caryophyllene oxide, the corresponding portion was estimated to be 14 %. Of the compounds that were completely lost (or below LOQ) in the online sampling, only 3-MA could not be detected in the empty tube run. If a clean sorbent tube was analyzed after online sampling instead of the empty tube used in the online sampling, no compounds were detected. Since the blank sorbent tube run after the online analysis did not show any analyte peaks, and yet the following empty tube analysis showed analyte peaks, it indicates that the lost analyte fraction is most likely lost partially into the empty tube and partially to TD parts/lines prior to the heated valve (Fig. S11).

In Fig. S12 are shown the recoveries obtained with three different empty stainless-steel (SS1-SS3) tubes used in online sampling mode. Overall, the recoveries of most MTs were acceptable with all three tubes (on average 96±6 %), except linalool recovery was fairly poor with two of the tubes (≈66 %) and with one tube linalool amount was below LOQ (Fig. S12). For almost all other analytes, mixed results were obtained with the different empty tubes tested. Sesquiterpenes (excluding β-farnesene) recoveries were satisfactory with two of the tubes tested (84±10 %), but with one of the tubes the SQTs recoveries were extremely poor (<25 %). Most notably, diterpenes were not observed in the online samples with any of the tubes tested. The empty tube cleaning (ultrasonication in methanol for 60 min and drying at 300 °C for 30 min) did not improve the online sampling performance. With some of the compounds, the recovery improved in consecutive repetitions, e.g. with linalool, bornylacetate and α-humulene the recoveries increased from 50 to 87 %, from 67 to 107 % and from 41 % to 105 %, respectively (between the first and second repetition).

Based on these results it can be concluded that β-farnesene, all DTs and caryophyllene oxide were commonly lost in significant amounts in online sampling. These compounds were lost at least partially into the inner surface of the empty stainless-steel tubes used for connecting online sampling box to the main TD. However, a significant fraction of the losses were not recovered by the re-analysis of the empty tubes, which indicates that those compounds are either totally lost into the tubes or losses are also occurring in the other parts of the TD unit.
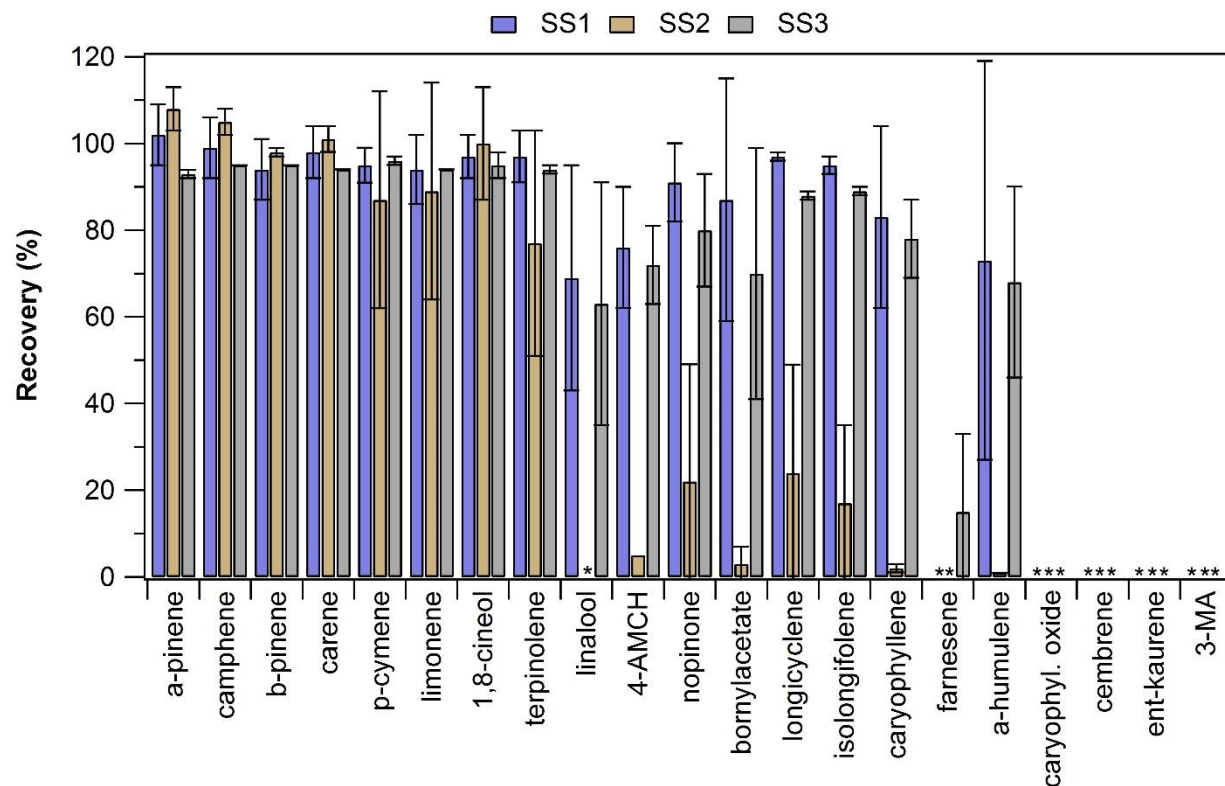
Figure S12. Recoveries obtained with three different empty stainless-steel (SS) tubes tested in online sampling. The error bars represent repeatability (*n*=2). The empty spaces marked with asterisk are results where the online sampling analyte concentrations were <LOQ.

S.1.3 Glass tube in online sampling

Since poor recoveries were observed with the stainless-steel empty tubes, an empty glass tube (from PerkinElmer Inc., Waltham, MA, USA) was tested in the online sampling mode. In general, the recovery results (Fig. S13) obtained with the empty glass tube were much better when compared to the results obtained with stainless-steel tubes. The recoveries of monoterpenoids and sesquiterpenes were acceptable, on average 85±6 % and 80±3 %, respectively (Fig. 13). Even β-farnesene could be detected and the recovery was 85±2 %; a notable improvement to previous online sampling mode results (Fig. S12). Furthermore, with the glass tube, caryophyllene oxide and DTs could be detected, however, the recoveries were still fairly poor (on average from 19±16 % to 81±66 %). With those compounds, the recoveries were improving in consecutive repetitions (*n*=4), e.g. with ent-kaurene from 16 % to 63 % and with cembrene from <LOQ to 156 %. Overall, the results obtained with the glass tube were promising, especially when compared to the results obtained previously with the stainless-steel tubes.
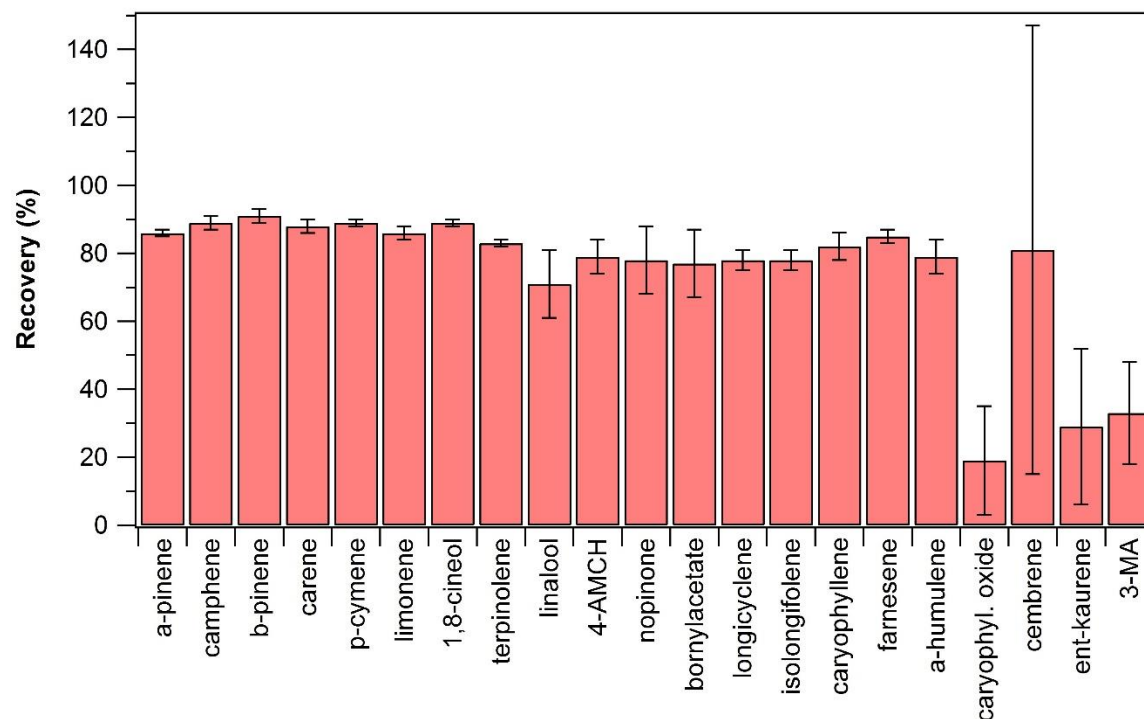
Figure S13. Recovery results obtained when empty glass tube was used in online sampling. The error bars represent repeatability (*n*=4).

S1.4 Effect of relative humidity

The effect of relative humidity (RH) on recoveries was tested with both empty stainless-steel tube and glass tube. Three different RH levels were tested (5 %, 40 % and 70 %). With each RH level, two repetitions were done.

The recovery results for both empty tube materials are shown in Fig. S14. With both tubes, the MTs recovery levels decreased slightly as the RH increased, e.g. with the stainless-steel tube the recoveries were on average 94±12 %, 89±6 % and 86±3 % at RH=5 %, RH=40 % and RH=70 %, respectively, although the difference in decline is within the standard deviation. With the stainless-steel tube, most sesquiterpenes recoveries stayed fairly constant at different RH levels (82±9 % at RH=5 %, 84±3 % at RH=40 % and 82±1 % at RH=70 %), except with β-farnesene which had an increasing recovery as the RH increased (Fig. S14a). Clearly, the increased RH level affected positively to the online sampling efficiency of β-farnesene with the stainless-steel tube. With the empty glass tube, the sesquiterpenes recoveries decreased slightly as the RH increased, on average from 90±4 % to 82±5 % (Fig. S14b). In general, with the glass tube, almost all other compounds showed either slightly decreasing recovery trend or the recoveries stayed fairly constant as the RH increased, except DTs and caryophyllene oxide. These compounds showed higher recoveries as the RH increased (on average recoveries increased from 21±14 % to 51±20 %, Fig. S14b). Similar trend was noticed with the stainless-steel tube, DTs and caryophyllene oxide recoveries increased from not detected to 15±17 % as the RH increased (most notably with caryophyllene oxide, Fig. S14a). Collectively, the results indicate that the compound losses in online sampling mode are lower when the sample air RH is higher.
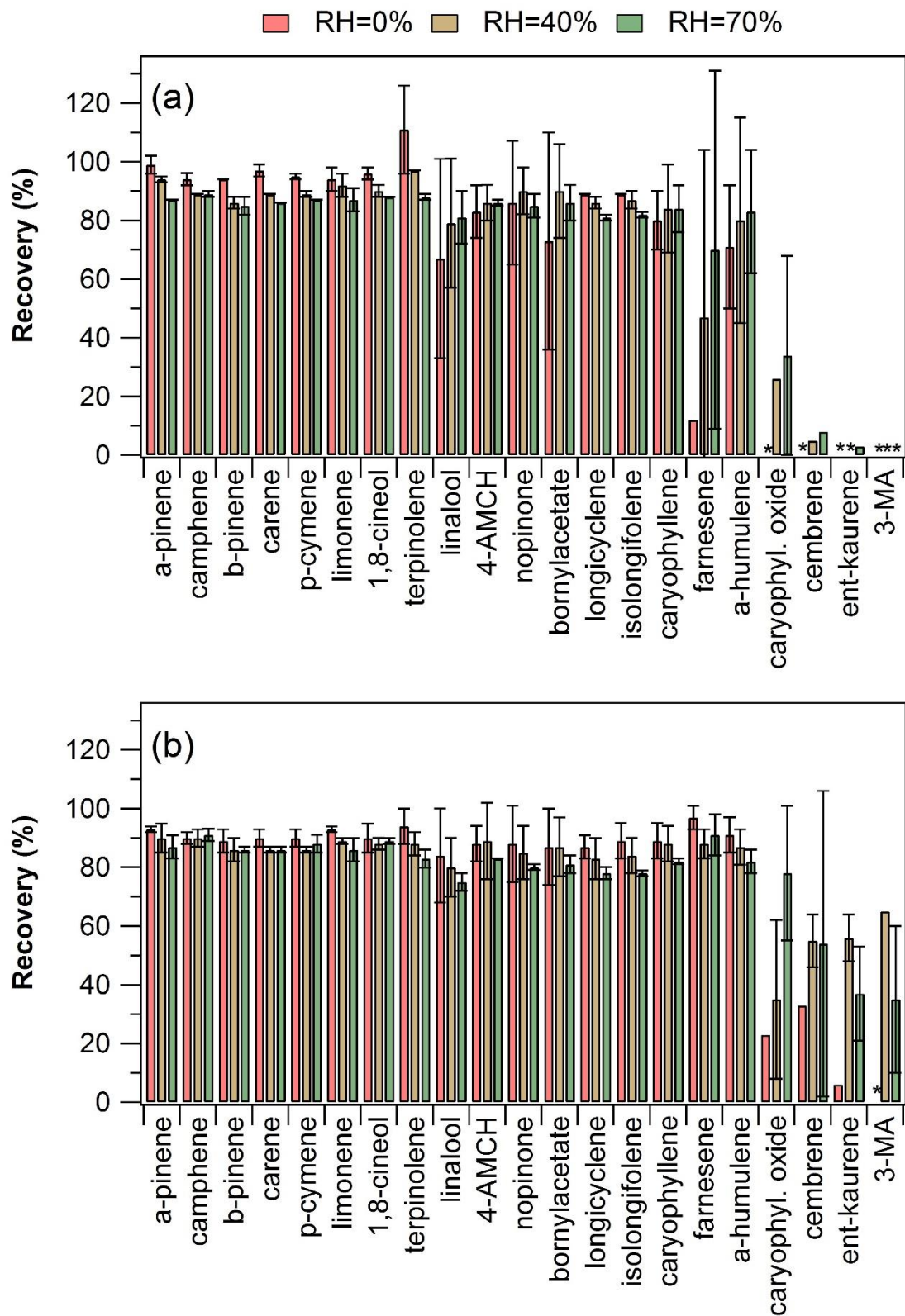
Figure S14. The effect of relative humidity (RH=0, 40 and 70 %) on analyte recoveries when using **(a)** stainless-steel empty tube or **(b)** glass tube. The error bars represent repeatability (*n*=2). The empty places marked with asterisk indicate online mode results <LOQ.

S1.5 TD unit line replacements

Since a fairly large portion of the losses of some compounds could not be explained by the empty tube accounted losses, some of the TD unit lines were replaced. As presented in Fig. S11, the online sample goes normally through a Nafion drier installment. In our TD unit, this was modified already from the beginning so that the Nafion dryer was replaced with a short piece of Teflon tubing. This setup was now further changed so that the lines between the connections and valves were changed from stainless-steel to Teflon tubing and the lines were made generally shorter. Specifically, the line from sample inlet to valve 1 and the line from valve 1 to valve 2 were replaced (Fig. S11). The other lines could not be easily changed and these were left as such (original stainless-steel tubing).

Unfortunately, the line replacements caused initially a general overall decrease in recoveries (data not shown). During first set of repetitions (with stainless-steel empty tube used in online sampling), even the MTs recoveries were fairly poor (on average 73±12 %). In general, the recoveries were roughly on average 10-20 % lower after the TD lines were changed from stainless-steel to Teflon tubing. However, over time when the experiments were repeatedly performed, the recoveries started to improve and eventually reached a similar level as prior to the line changes (Fig. S15). In fact, the recoveries of caryophyllene oxide and DTs were slightly better after the line changes than prior to line changes.
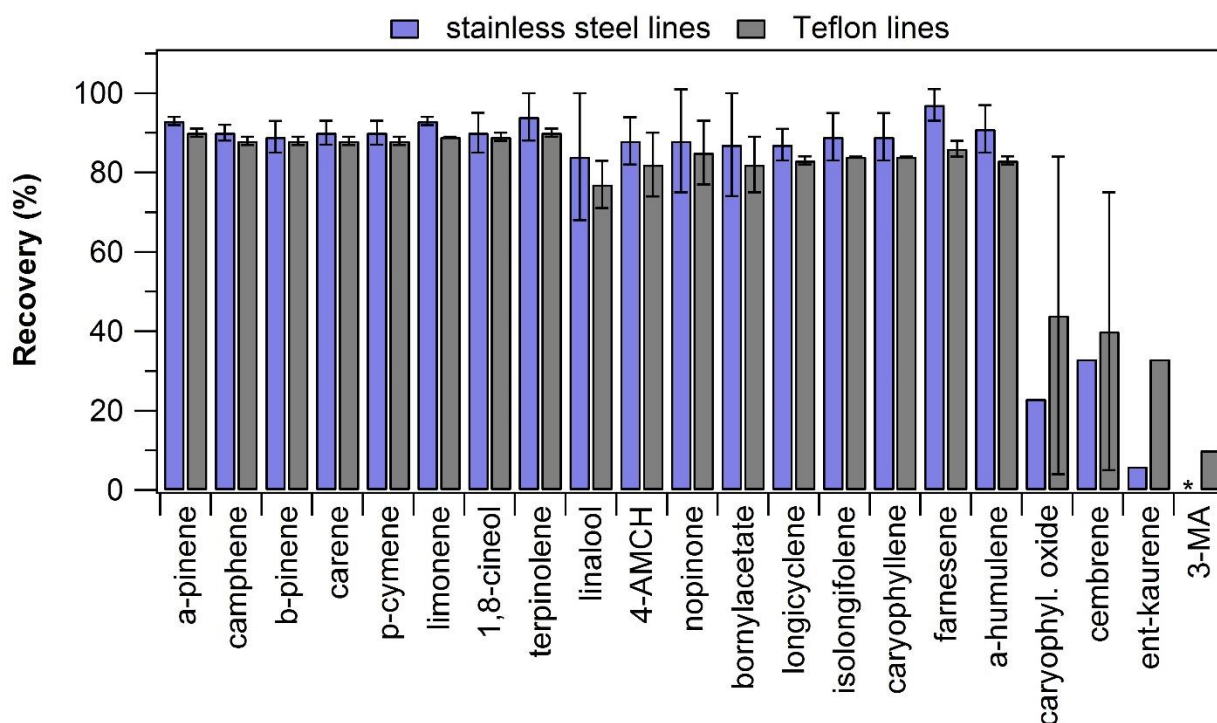
Figure S15. The results obtained after the TD unit line changes from stainless-steel lines to Teflon lines. Experiments were performed at RH=0 % by using an empty glass tube in online sampling. Error bars represent repeatability (*n*=2). The empty spaces marked with asterisk indicate online mode results <LOQ.

S1.6 Recoveries with an empty glass coated stainless-steel tube

According to TD-GC-MS manufacturers' recommendation (personal communication), an empty stainless-steel tube with glass coated inner surface (from PerkinElmer Inc., Waltham, MA, USA) was tested in online sampling. This glass coated stainless-steel tube was reportedly better in terms of robustness when compared to the plain glass tube. In addition, it was speculated that the glass coated stainless-steel tube

might work better in online sampling than the plain glass tube due to slightly higher tube temperature. In online sampling mode, the empty tube is theoretically at room temperature during sampling, however, the upper part of the tube is connected to the heated valve via a fixed metallic tube holder (Fig. S11). Thus, in practice the heat was transferred through the metal parts to the upper part of the tube and the stainless-steel tube was unintentionally slightly heated. Since heat is beneficial for avoiding terpene losses, it was speculated that the difference between the plain glass and glass coated stainless-steel tube might be observable due to the difference in material heat transfer capability.

As can be seen Fig. S16, the recoveries were on a similar level with the glass coated stainless-steel tube and with the previously tested plain glass tube. The speculated improved heat transfer effect did not seem to affect the recoveries in reality. Both empty tubes that had glass inner surface performed generally better than the stainless-steel tube in online sampling. This was especially the case in the recoveries of β-farnesene, DTs and caryophyllene oxide (Fig. S16).
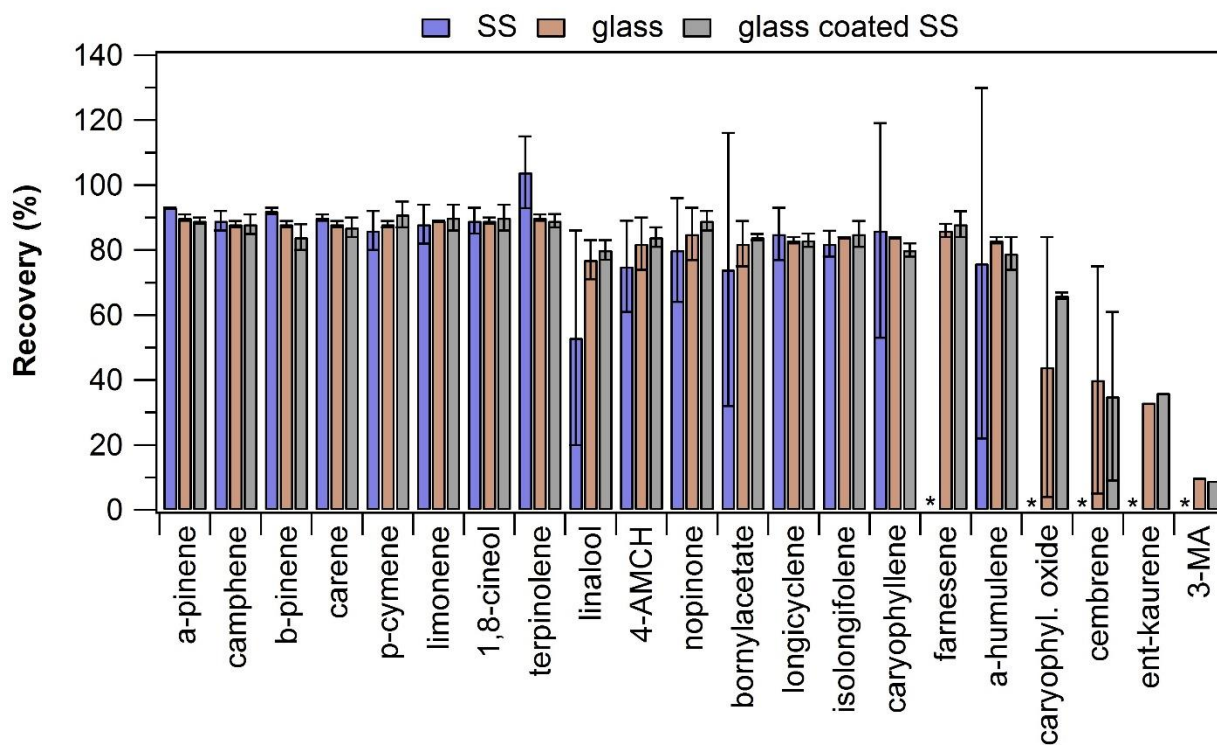
Figure S16. Comparison of the recovery levels obtained when using either stainless-steel (SS), glass tube or glass inner surface coated stainless-steel tube in online sampling at RH=0 %. The error bars represent repeatability (*n*=2). The empty spaces marked with asterisk indicate online mode results <LOQ.

The effect of RH on recoveries from the glass coated stainless-steel tube (Fig. S17) was similar as previously with the plain glass tube (Fig. S14b). The recoveries of DTs and caryophyllene oxide increased as the RH increased. It seems that if the RH is high enough, the online sampling agrees fairly well with the offline sampling results.
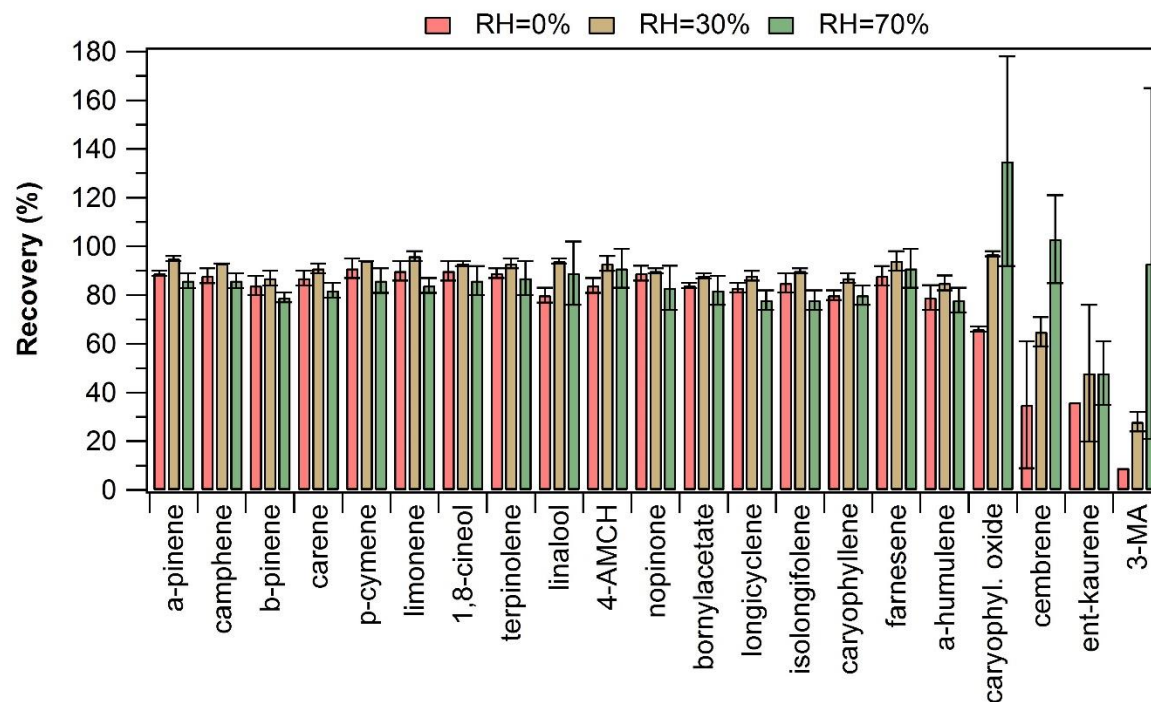
Figure S17. Effect of relative humidity (RH) on recoveries when the glass coated empty stainless-steel tube was used in online sampling. The error bars represent repeatability (*n*=2-3).

S1.7 Summary of results

The comparison of results obtained by online and offline mode sampling revealed that some compounds were partially lost in the online sampling. In general, the losses were compound specific and mainly restricted to β-farnesene, caryophyllene oxide and DTs. Monoterpenoids and other sesquiterpenes results agreed fairly well between both sampling modes. The main parameters observed to affect the recoveries of SQTs and DTs were sample air relative humidity and the material of the empty tube used in online sampling (or materials in general in the sample air path). Empty tubes made of glass performed better than stainless-steel tubes in online sampling. When the glass tubes were used in online sampling, β-farnesene had acceptable recovery (≈87 %). Also, with the glass tubes diterpenes and caryophyllene oxide could be detected, and at high RH level the recoveries were on average satisfactory (≈64 %), although the uncertainties in results were substantial. With stainless-steel tubes, the recoveries of DTs were poor (<35 %) even at the highest RH level.

Our tentative results indicated that in long-term use of online sampling the recoveries may stabilize and improve. We had on maximum four consecutive repetitions, which showed improvement in recoveries of some of the compounds. However, this should be studied further in future with more repetitions.

In summary, online TD-GC-MS sampling and analysis can be used for the quantification of monoterpenoids and sesquiterpenes in air samples. However, the quantification of DTs and caryophyllene oxide can be challenging. Based on the results presented here, it is recommended to use empty tubes which have glass inner surface in online sampling. In addition, the sample air relative humidity should be controlled (if possible) and monitored. Since the relative humidity seemed to have an effect on online sampling performance of DTs and caryophyllene oxide, it might be necessary to derive correction equation experimentally to harmonize the results if the RH changes in sample air.
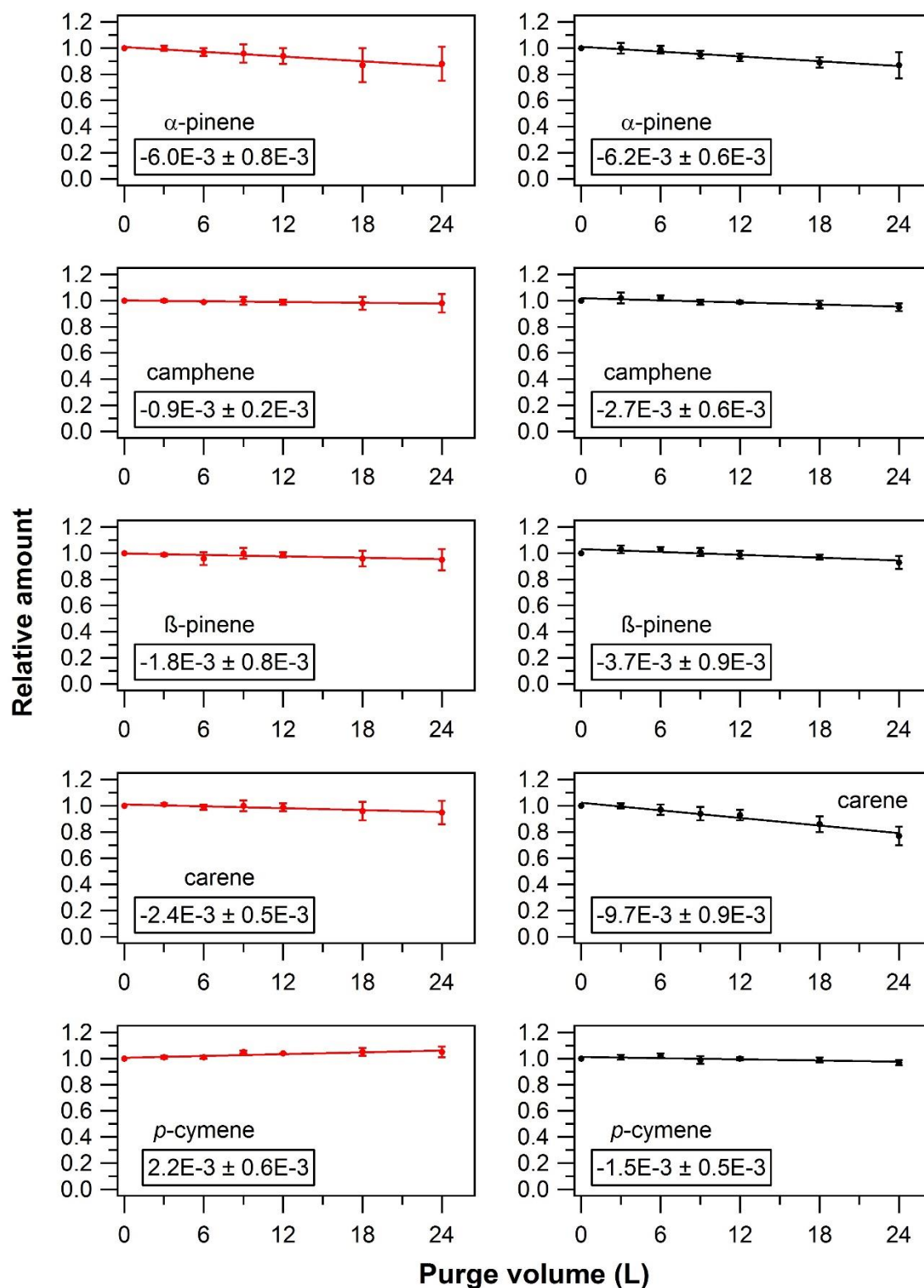
Figure S18. Results from the ozone exposure experiments. The left (red) and right (black) panel plots are from the O_3=0 ppb and O_3=40 ppb experiments, respectively. The values embedded into the plots are the slopes (±uncertainty) of the linear regression fits. The error bars represent reproducibility (*n*=3).
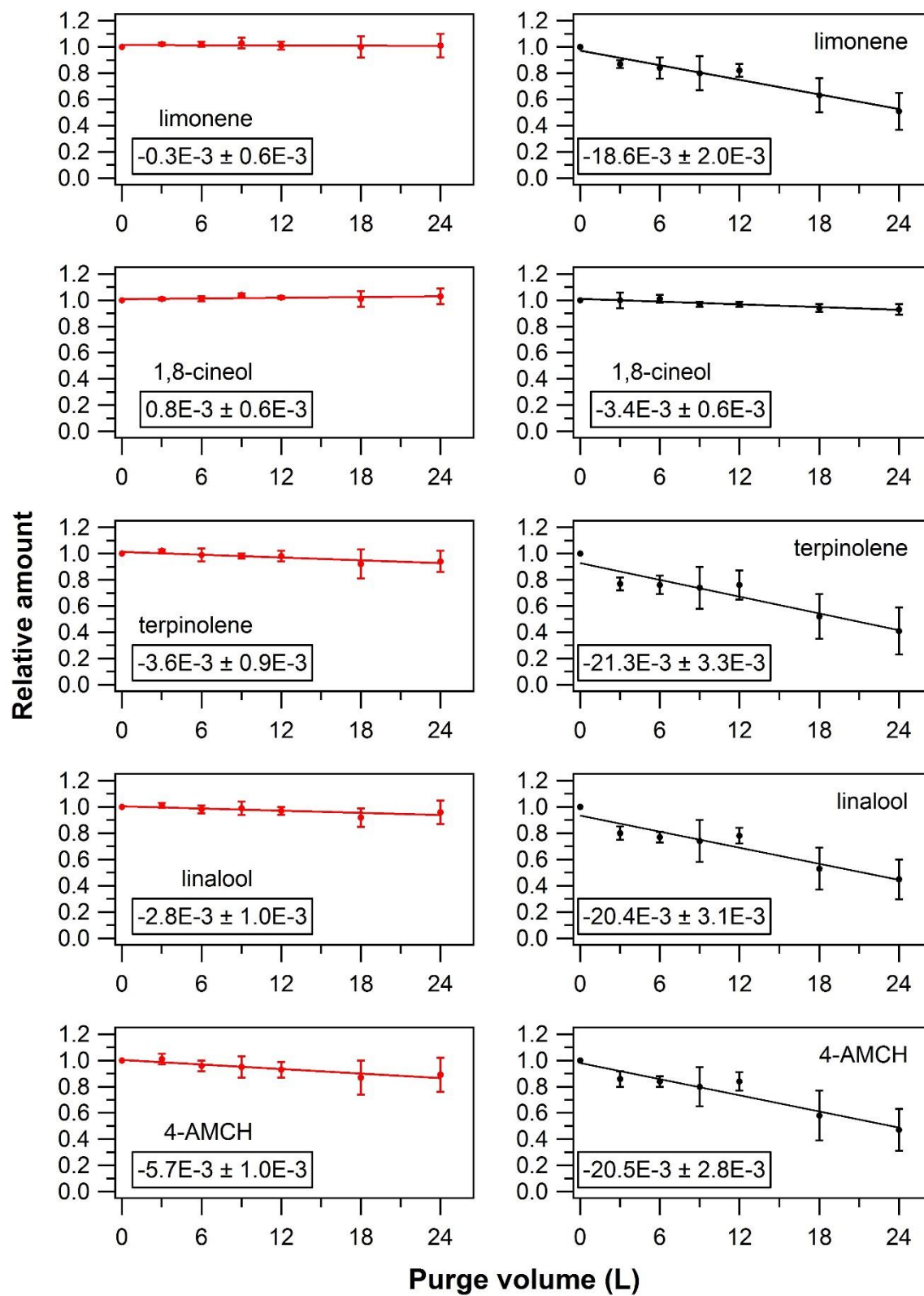
Figure S18. (continued)
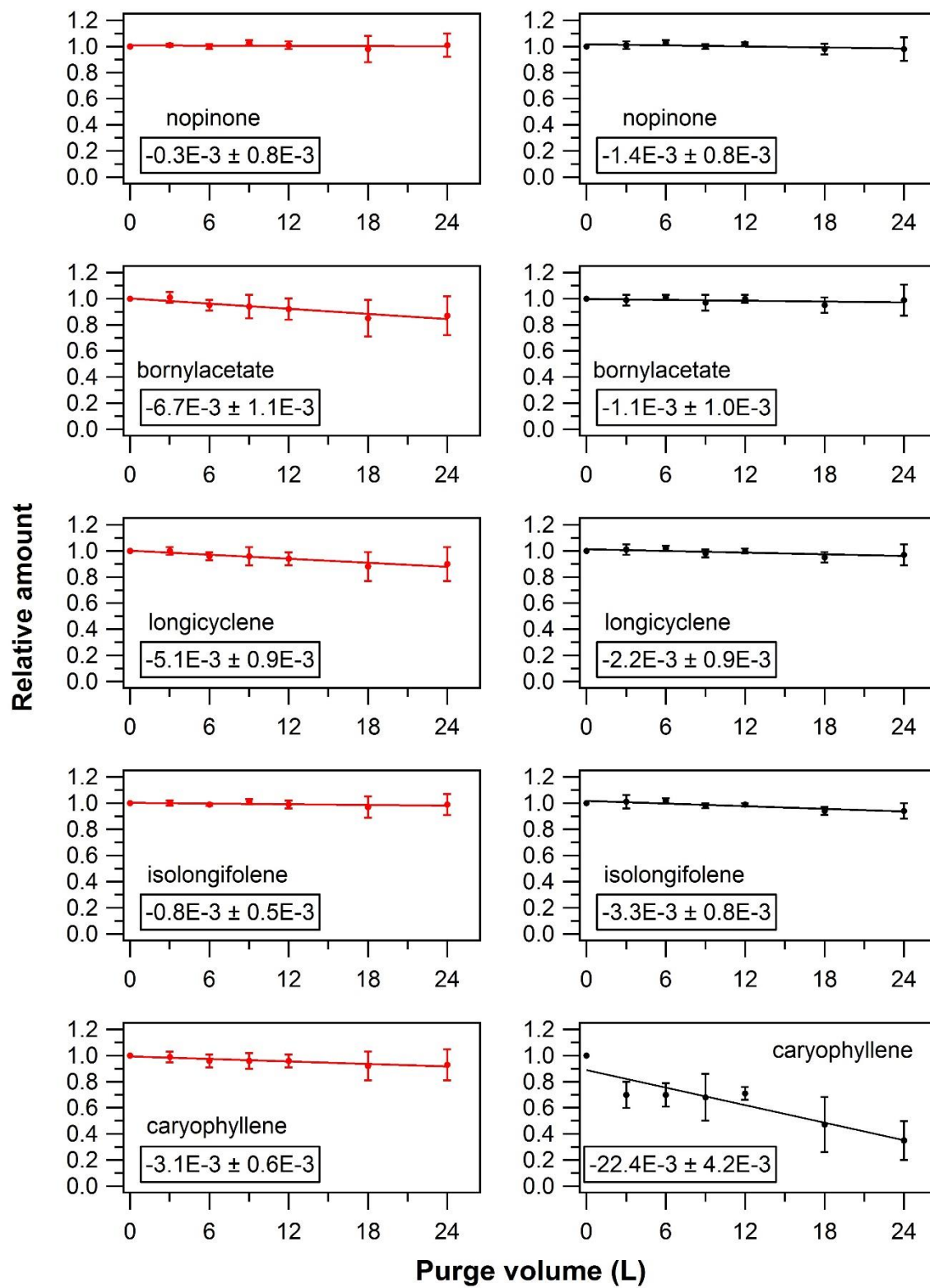
Figure S18. (continued)
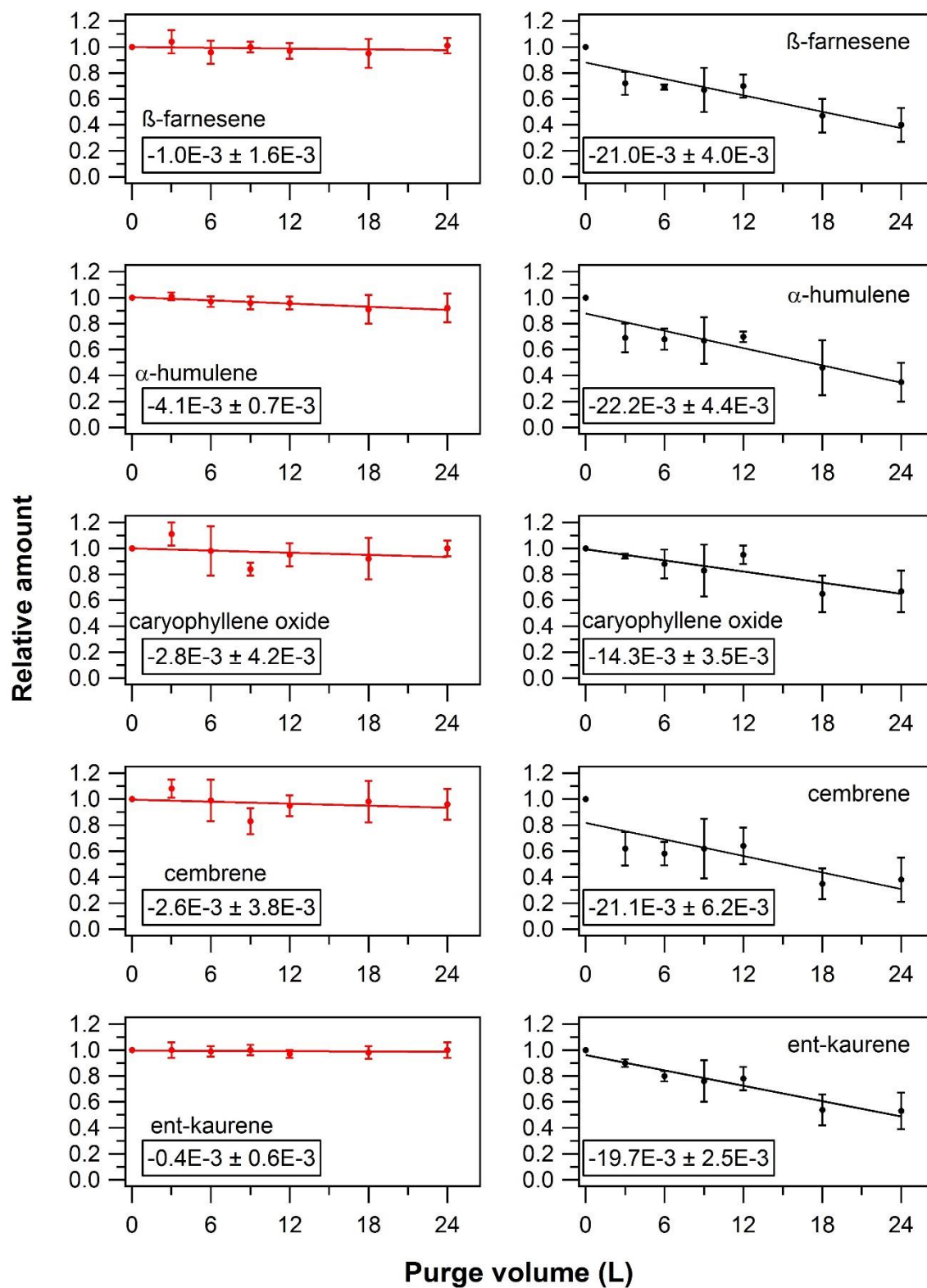
Figure S18. (continued)
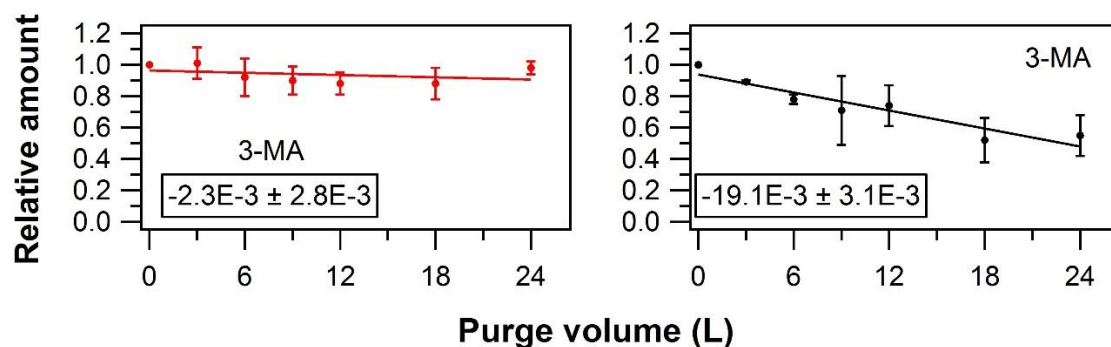
Figure S18. (continued)

Table S3. Literature retrieved k_{O3} values and the estimated k_{O3} values obtained based on main text Fig. 4 linear regression fit.

Compound	k_{O3} literature (cm³/molecule*s)	Reference	k_{O3} estimated (cm³/molecule*s)
α-pinene	$9.6*10^{-17}$	IUPAC[a]	$(1.6\pm3.8)*10^{-17}$
camphene	$5.0*10^{-19}$	IUPAC	$(5.1\pm8.7)*10^{-18}$
β-pinene	$1.9*10^{-17}$	IUPAC	$(7.7\pm14.8)*10^{-18}$
3-carene	$4.9*10^{-17}$	IUPAC	$(5.2\pm15.7)*10^{-17}$
p-cymene	-	-	$(3.4\pm5.4)*10^{-18}$
limonene	$2.2*10^{-16}$	IUPAC	$(9.2\pm51.1)*10^{-16}$
1,8-cineol	-	-	$(6.6\pm12.1)*10^{-18}$
terpinolene	$1.6*10^{-15}$	IUPAC	$(2.6\pm17.5)*10^{-15}$
linalool	-	-	$(1.8\pm11.1)*10^{-15}$
4-AMCH	-	-	$(1.8\pm11.5)*10^{-15}$
nopinone	-	-	$(3.4\pm5.3)*10^{-18}$
bornylacetate	-	-	$(2.9\pm4.4)*10^{-18}$
longicyclene	-	-	$(4.4\pm7.3)*10^{-18}$
isolongifolene	$1.0*10^{-17}$	IUPAC	$(6.6\pm12.1)*10^{-18}$
β-caryophyllene	$1.2*10^{-14}$	IUPAC	$(3.4\pm23.9)*10^{-15}$
β-farnesene	$5.6*10^{-16}$	IUPAC	$(2.1\pm13.3)*10^{-15}$
α-humulene	$1.2*10^{-14}$	IUPAC	$(3.1\pm21.7)*10^{-15}$
caryophyllene oxide	$1.2*10^{-17}$	EPISuite[b]	$(2.6\pm10.9)*10^{-16}$
cembrene	$1.9*10^{-15}$	EPISuite	$(2.3\pm15.5)*10^{-15}$
ent-kaurene	$1.2*10^{-17}$	EPISuite	$(1.4\pm8.2)*10^{-15}$
3-MA	-	-	$(1.1\pm6.5)*10^{-15}$

[a] IUPAC Task Group on Atmospheric Chemical Kinetic Data Evaluation (http://iupac.pole-ether.fr)
[b] EPISuite, Environmental Protection Agency, United States (https://www.epa.gov/tsca-screening-tools)
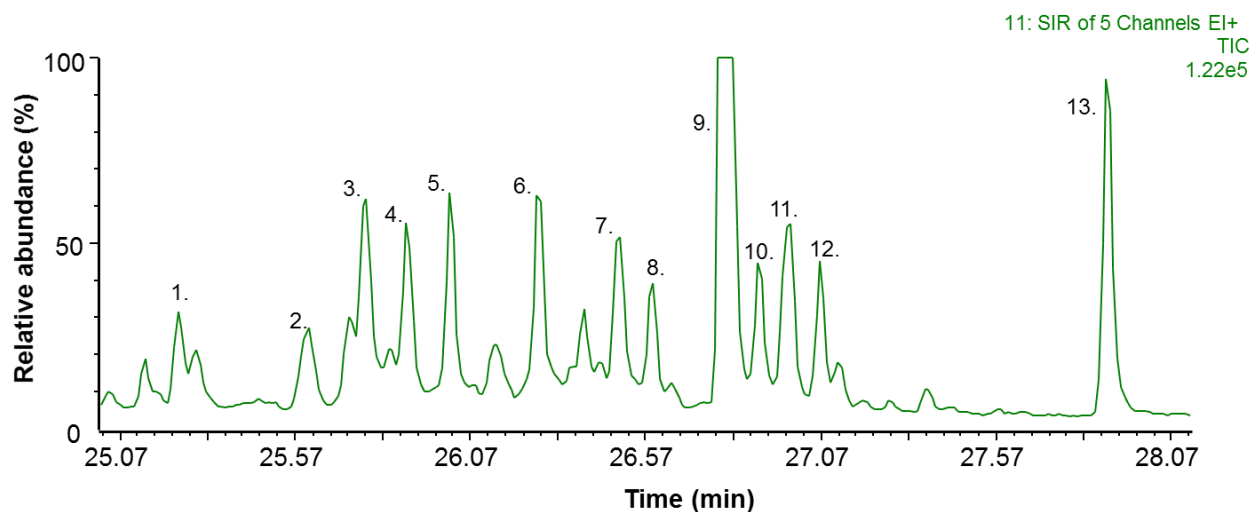
Figure S19. Selected ion recording (SIR) chromatogram from the TD-GC-MS1 analysis of pine needles purge-and-trap sorbent tube sample (sampling at 60 °C for 20 min at a flow rate of 100 mL/min). The five m/z ions included in the SIR were m/z 93, 229, 257, 272 and 275. The chromatogram is scaled for presentation purposes, peak number 9 is not showed in full height in order to visualize the other peaks more clearly. Peak identification: 1. Unidentified ($C_{19}H_{30}$), 2. Unidentified ($C_{19}H_{28}$), 3. Unidentified ($C_{18}H_{26}O$), 4. Unidentified ($C_{19-20}H_{32}O_{0-2}$), 5. Unidentified ($C_{20}H_{32}$), 6. Sandaracopimaradiene, 7. Unidentified ($C_{19-20}H_{28}O_{0-1}$), 8. Unidentified ($C_{20}H_{30-32}O_{0-2}$), 9. 13-epi-manool oxide, 10. Unidentified ($C_{19-20}H_{28-32}O_{0-1}$), 11. Unidentified ($C_{19-20}H_{28}O_{0-1}$), 12. Unidentified ($C_{20}H_{34}O$) and 13. Abietadiene. See Table S4 for further information on peak identification.
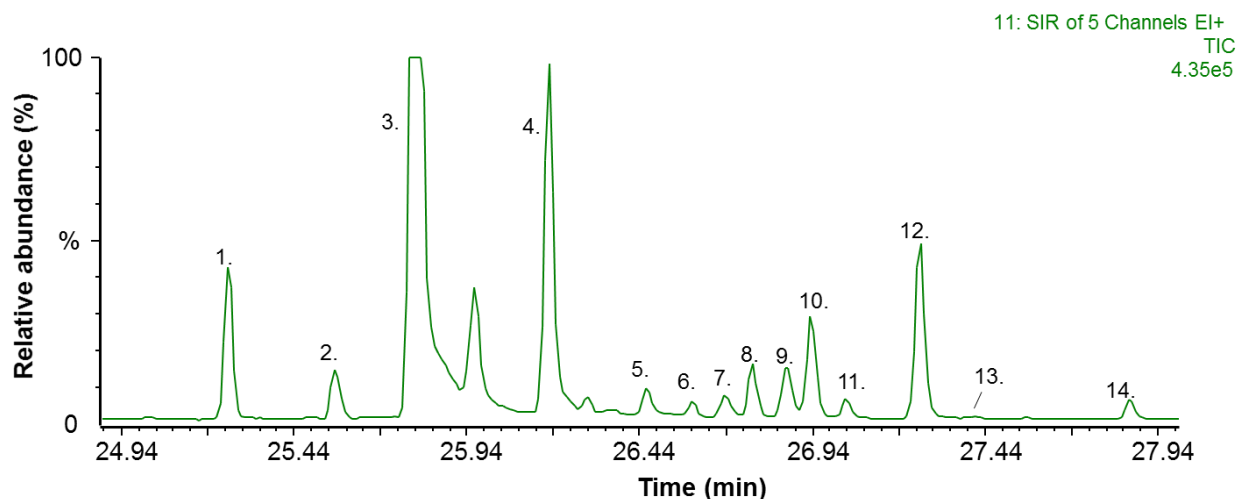
Figure S20. Selected ion recording (SIR) chromatogram from the TD-GC-MS1 analysis of spruce twigs dynamic headspace sorbent tube sample (sampling at 60 °C for 20 min at flow rate of 100 mL/min). The five m/z ions included in the SIR were m/z 93, 229, 257, 272 and 275. The TIC is scaled for presentation purposes, peak number 3 is not showed in full height in order to visualize the other peaks more clearly. Peak identification: 1. Rimuene, 2. Unidentified ($C_{20}H_{32}$), 3. Cembrene, 4. Cembrene A, 5. Unidentified ($C_{20}H_{32}$), 6. Unidentified ($C_{20}H_{32}$), 7. Unidentified ($C_{20}H_{32}$), 8. 13-epi-manool oxide, 9. Unidentified ($C_{20}H_{32}$), 10. Unidentified ($C_{19-20}H_{28-30}$), 11. Unidentified ($C_{20}H_{34}O$), 12. Unidentified ($C_{20}H_{32}$), 13. Abietatriene and 14. Unidentified ($C_{20}H_{32}$). See Table S4 for further information on peak identification.

Table S4. Tentative identification of diterpenoids and alike compounds in dynamic headspace samples of pine needles and spruce twigs.

Sample	Peak no.[a]	RI[b]	Formula[c]	CAS	Name or m/z peaks[d]
pine	1	1914 (1914)	$C_{19}H_{30}$	-	243, 123, 133, 258
	2	1944 (1943)	$C_{19}H_{28}$	-	91, 79, 241, 256
	3	1957 (1957)	$C_{18}H_{26}O$	-	123, 81, 243, 258
	4	1966 (1966)	$C_{19-20}H_{32}O_{0-2}$	-	81, 178, 243, 261
	5	1977 (1976)	$C_{20}H_{32}$	-	257, 243, 272, 79
	6	1997 (1997)	$C_{20}H_{32}$	1686-56-2	sandaracopimaradiene
	7	2016 (2016)	$C_{19-20}H_{28}O_{0-1}$	-	159, 241, 185, 256
	8	2025 (2025)	$C_{20}H_{30-32}O_{0-2}$	-	91, 134, 92, 123
	9	2043 (2042)	$C_{20}H_{34}O$	1227-93-6	13-epi-manool oxide
	10	2051 (2050)	$C_{19-20}H_{28-32}O_{0-1}$	-	79, 91, 105 272
	11	2058 (2058)	$C_{19-20}H_{28}O_{0-1}$	-	159, 241, 185, 256
	12	2065 (2064)	$C_{20}H_{34}O$	-	257, 275, 81, 69
	13	2136 (2136)	$C_{20}H_{32}$	35241-40-8	abietadiene
spruce	1	1914 (1914)	$C_{20}H_{32}$	1686-67-5	rimuene
	2	1940 (1940)	$C_{20}H_{32}$	-	257, 272, 67, 81
	3	1958 (1958)	$C_{20}H_{32}$	1898-13-1	cembrene
	4	1990 (1989)	$C_{20}H_{32}$	71213-92-8	cembrene A
	5	2014 (2014)	$C_{20}H_{32}$	-	137, 136, 91, 257
	6	2025 (2025)	$C_{20}H_{32}$	-	120, 106, 133, 272
	7	2033 (2032)	$C_{20}H_{32}$	-	136, 121, 93, 272
	8	2040 (2040)	$C_{20}H_{34}O$	1227-93-6	13-epi-manool oxide
	9	2048 (2047)	$C_{20}H_{32}$	-	119, 93, 257, 272
	10	2054 (2053)	$C_{19-20}H_{28-30}$	-	159, 257, 241, 272
	11	2062 (2062)	$C_{20}H_{34}O$	-	257, 275, 123, 147
	12	2081 (2081)	$C_{20}H_{32}$	-	81, 229, 257, 272
	13	2094 (2094)	$C_{20}H_{30}$	19407-28-4	abietatriene
	14	2133 (2133)	$C_{20}H_{32}$	-	272, 55, 96, 131

[a] Peak number marked in Figs. S19 and S20.

[b] Retention index (RI) values presented as Kovats index (and arithmetic index in brackets).

[c] Proposed or tentatively identified formula of the compound.

[d] The presented m/z ions are either the most abundant ions or m/z ions considered to be characteristic for the specific peak. The underlined m/z ion is the most abundant one.
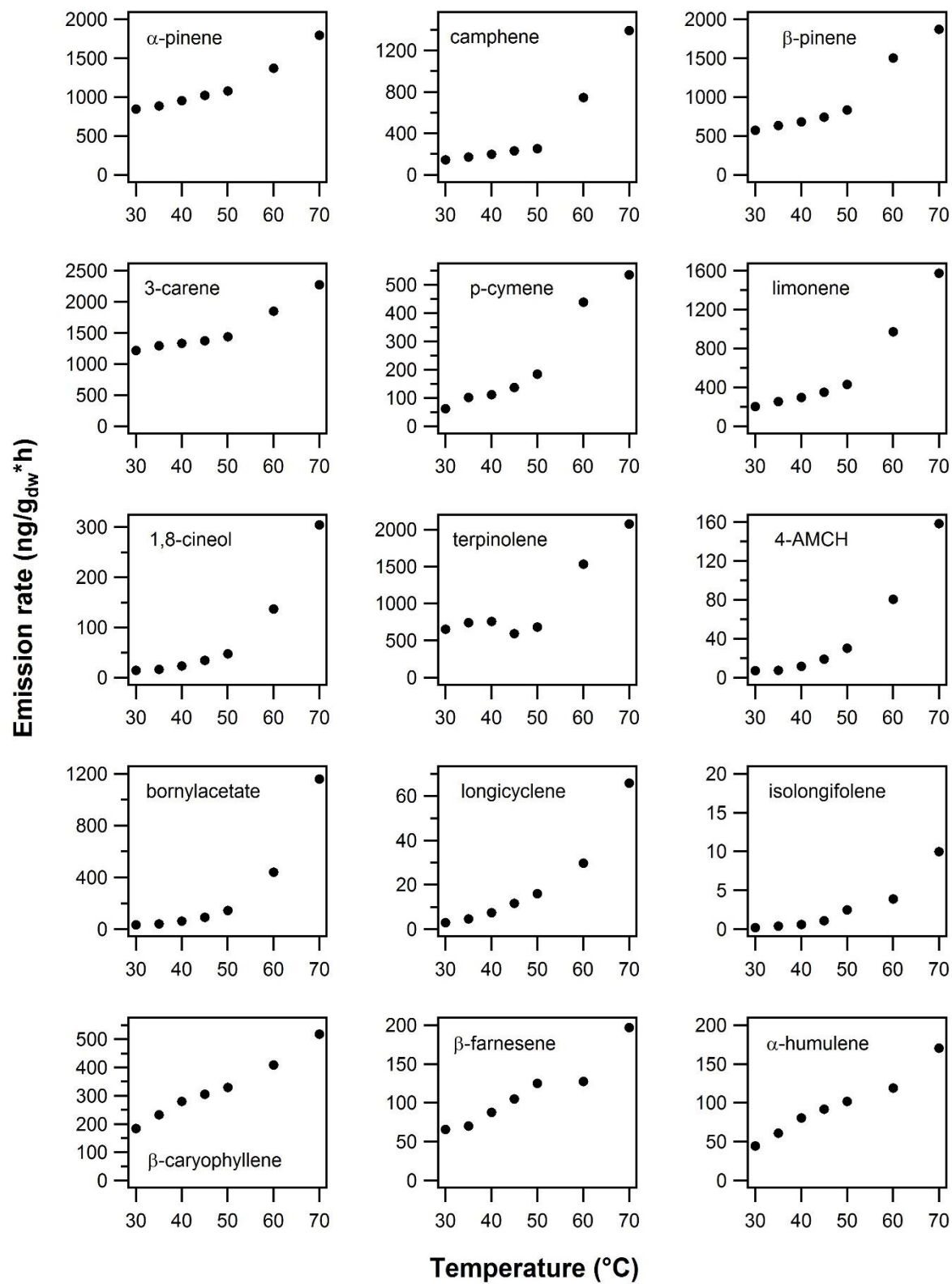
Figure S21. Terpenoid emission rates from pine needles as a function of oven temperature in the dynamic headspace extraction experiments.
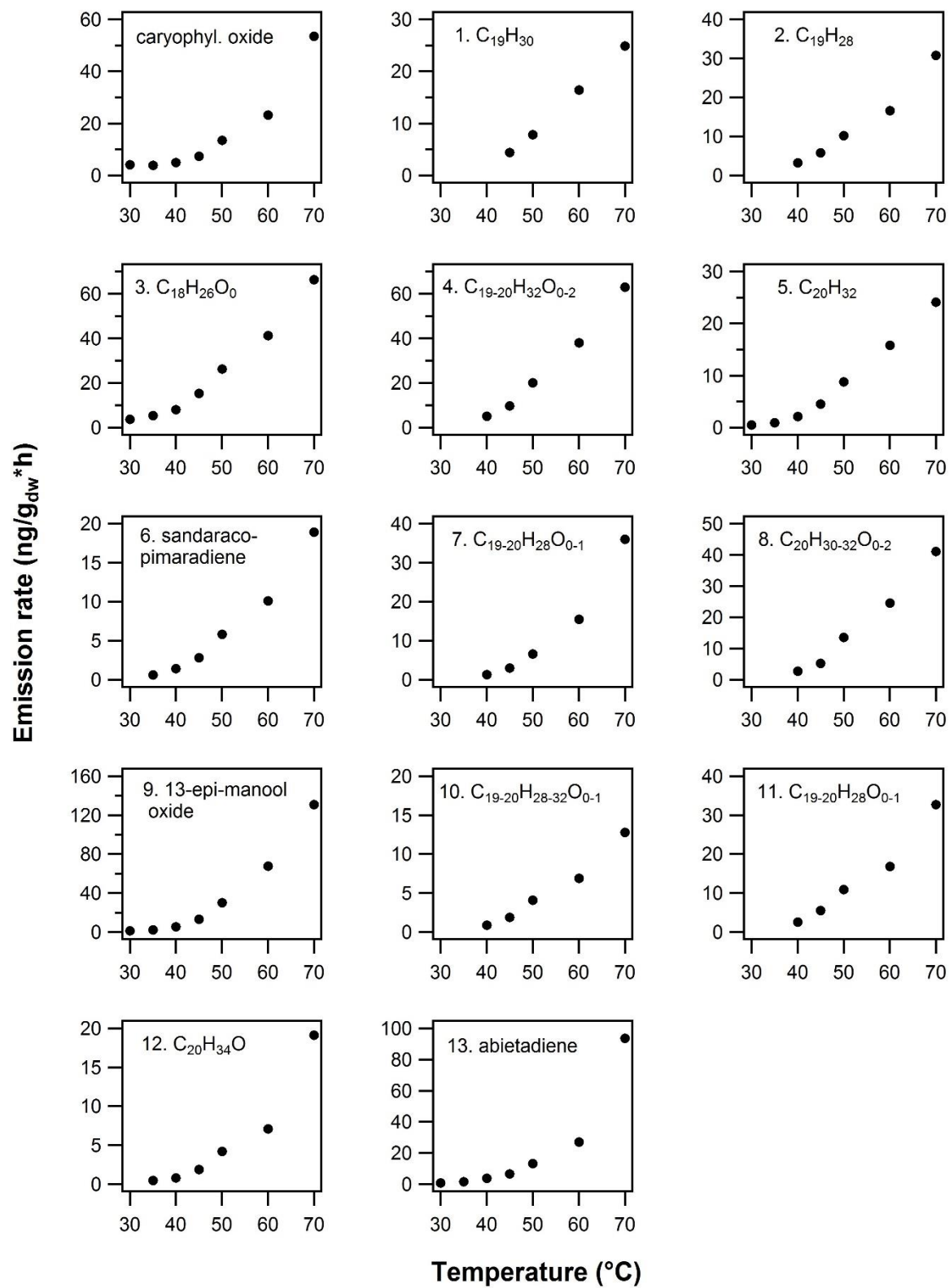
Figure S21. (continued)
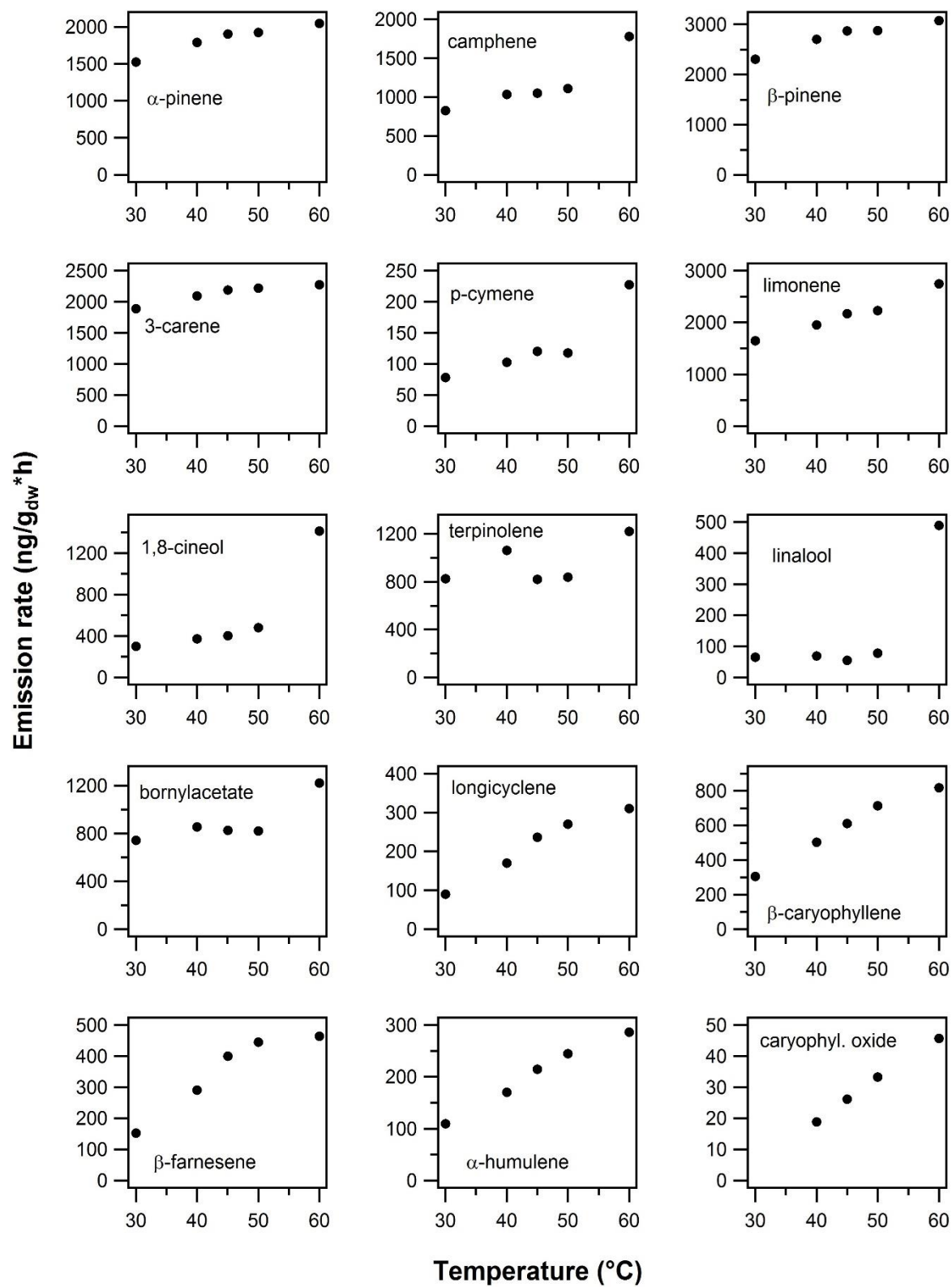
Figure S22. Terpenoid emission rates from spruce twigs as a function of oven temperature in the dynamic headspace extraction experiments.

Emission rate (ng/g$_{dw}$*h)

Temperature (°C)
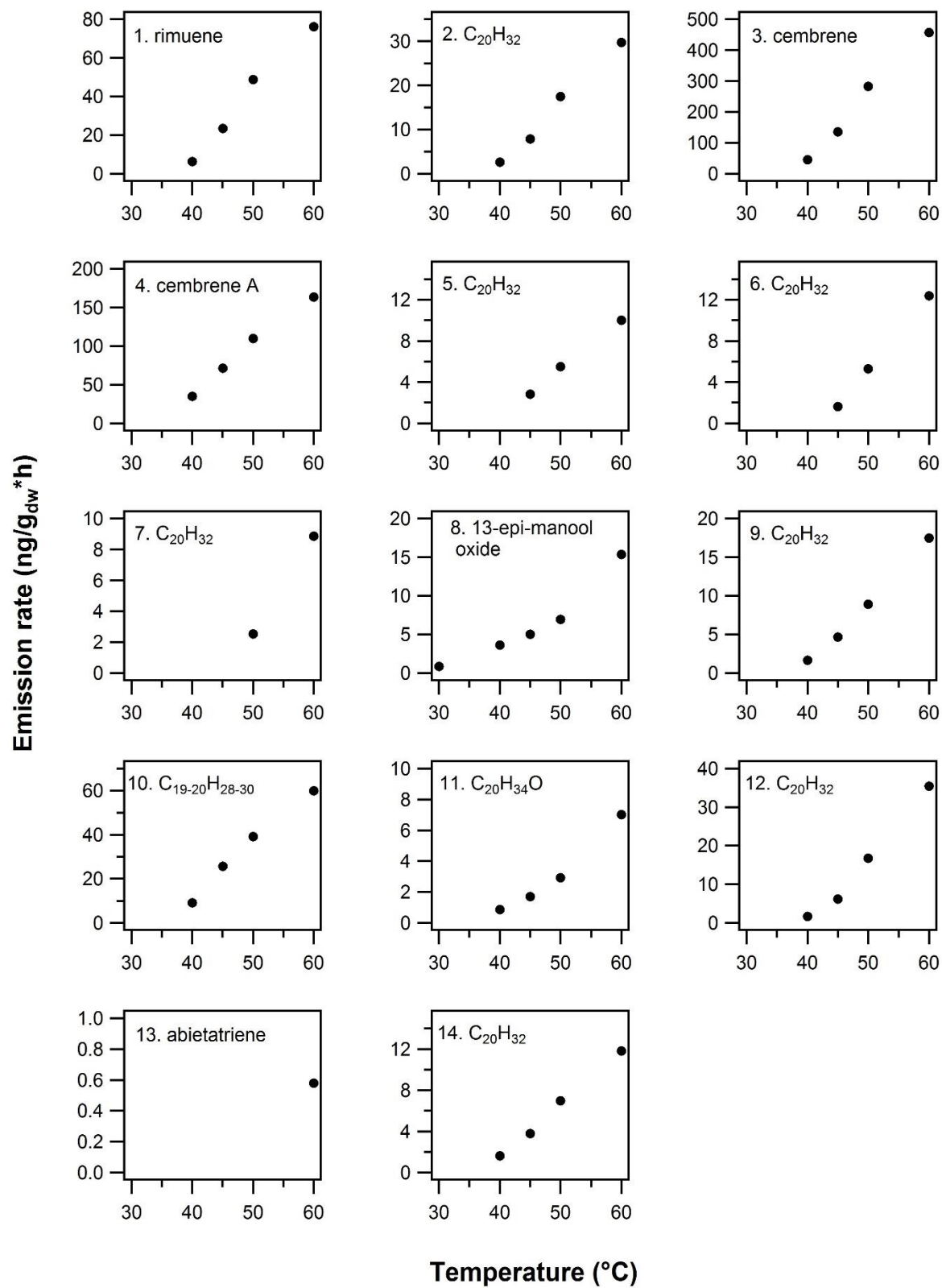
Figure S22. (continued)

Table S5. Results from the spruce branch enclosure experiments.

KI^a	AI^b	Formula^c	CAS	Name or m/z peaks^d	Emission rate^e (ng/g$_{dw}$*h)	Emission rate^f (ng/g$_{dw}$*h)
943±1	940±1	$C_{10}H_{16}$	7785-70-8	α-pinene	3630±239	5674±373
961±1	958±1	$C_{10}H_{16}$	79-92-5	camphene	1797±118	5048±332
981±1	979±1	$C_{10}H_{16}$	3387-41-5	sabinene	589±39	1449±95
988±1	986±1	$C_{10}H_{16}$	19902-08-0	β-pinene	3975±261	6045±398
992±0	991±0	$C_{10}H_{16}$	123-35-3	myrcene	1999±131	3690±243
1014±1	1013±1	$C_{10}H_{16}$	99-83-2	α-phellandrene	246±16	1482±97
1018±1	1016±1	$C_{10}H_{16}$	498-15-7	3-carene	655±43	1304±86
1033±1	1030±1	$C_{10}H_{14}$	99-87-6	*p*-cymene	385±25	982±65
1039±1	1036±1	$C_{10}H_{16}$	5989-54-8	limonene	8722±574	19443±1279
1043±1	1040±1	$C_{10}H_{18}O$	470-82-6	1,8-cineol	9001±592	13276±873
1051±1	1048±1	$C_{10}H_{16}$	3338-55-4	β-ocimene	1523±100	3648±240
1067±0	1064±0	$C_{10}H_{16}$	99-85-4	γ-terpinene	2881±189	7296±480
1079±0	1077±0	$C_{10}H_{18}O$	-	93, 71, 121, 136	193±13	1201±79
1093±1	1092±1	$C_{10}H_{16}$	586-62-9	terpinolene	592±39	1452±95
1102±1	1102±1	$C_{10}H_{18}O$	78-70-6	linalool	2733±180	5266±346
1162±1	1160±1	$C_{10}H_{16}O$	76-22-2	camphor	14848±977	23930±1574
1170±1	1169±1	$C_{10}H_{18}O$	-	71, 136, 139, 154	4409±290	6486±427
1185±0	1184±0	$C_{10}H_{18}O$	507-70-0	borneol	24667±1623	43849±2884
1191±0	1190±0	$C_{10}H_{18}O$	562-74-3	terpinen-4-ol	4867±320	6779±446
1205±0	1204±0	$C_{10}H_{18}O$	98-55-5	α-terpineol	13494±888	18170±1195
1220±0	1219±0	$C_{10}H_{14}O$	80-57-9	verbenone	2451±161	4439±292
1229±1	1228±1	$C_{10}H_{20}O$	106-22-9	citronellol	4726±311	8600±566
1266±1	1265±1	$C_{10}H_{16}O$	89-81-6	piperitone	6317±416	9919±652
1294±1	1293±1	$C_{12}H_{20}O_2$	5655-61-8	bornylacetate	2976±196	6721±442
1348±1	1346±1	$C_{12}H_{20}O_3$	-	108, 71, 126, 212	128±8	1676±110
1355±0	1354±0	$C_{12}H_{20}O_2$	80-26-2	α-terpinyl acetate	1789±118	3812±251
1360±1	1359±1	$C_{10}H_{12}O_2$	97-53-0	eugenol	121±8	542±36
1370±1	1369±1	$C_{15}H_{24}$	5989-08-2	α-longipinene	325±21	744±49
1378±1	1377±1	$C_{11-12}H_{18-20}O_2$	-	69, 67, 93, 121	244±16	1375±90
1401±0	1401±0	$C_{11}H_{14}O_2$	-	178, 147, 163, 107	40±3	327±22
1423±0	1423±0	$C_{10}H_{16}O$	-	109, 67, 137, 152	-	624±41
1435±0	1434±0	$C_{15}H_{24}$	-	161, 105, 159, 204	230±15	668±44
1441±1	1440±1	$C_{15}H_{24}$	87-44-5	β-caryophyllene	100±7	686±45
1458±1	1457±1	$C_{15}H_{24}$	18794-84-8	β-farnesene	740±49	1122±74
1477±1	1477±1	$C_{15}H_{24}$	6753-98-6	α-humulene	102±7	179±12
1501±1	1501±1	$C_{15}H_{24}$	23986-74-5	germacrene D	330±22	694±46
1508±0	1508±0	$C_{15}H_{24}$	-	69, 93, 55, 119	118±8	414±27
1514±1	1513±1	$C_{15}H_{24}$	-	161, 105, 91, 204	100±7	459±30
1552±2	1551±2	$C_{15}H_{24}$	-	93, 121, 136, 204	732±48	987±65

KI[a]	AI[b]	Formula[c]	CAS	Name or m/z peaks[d]	Emission rate[e] $(ng/g_{dw}*h)$	Emission rate[f] $(ng/g_{dw}*h)$
1597±1	1597±1	$C_{15}H_{24}O_{0-1}$	-	159, 161, 105, 79	429±28	891±59
1607±1	1606±1	$C_{15}H_{24}O$	1139-30-6	caryophyllene oxide	-	423±28
1731±0	1730±0	$C_{15}H_{24}O$	-	177, 159, 131, 220	-	356±23
1757±1	1756±1	$C_{15}H_{26}O_2$	-	153, 135, 177, 238	377±25	1523±100
1786±2	1786±2	$C_{14}H_{12}O_2$	120-51-4	benzyl benzoate	605±40	1075±71
1840±0	1840±0	$C_{15}H_{24}O$	-	162, 55, 159, 220	-	239±16
1851±0	1850±0	$C_{15}H_{24}O$	-	159, 187, 220, 202	-	1108±73
1892±2	1892±2	$C_{14}H_{12}O_3$	118-58-1	benzyl salicylate	1010±66	1273±84
1909±1	1905±6	$C_{20}H_{32}$	1686-67-5	rimuene	38±3	462±30
1953±1	1952±1	$C_{20}H_{32}$	1898-13-1	cembrene	15±1	158±10
1959±0	1959±0	$C_{16}H_{30}O_2$	-	55, 69, 236, 254	14±1	244±16
1979±1	1979±1	$C_{20-22}H_{32-36}O_{0-2}$	-	55, 106, 257, 272	5±0	69±5
2015±1	2015±1	$C_{20}H_{32}$	-	120, 106, 133, 272	11±1	318±21
2070±0	2069±0	$C_{20}H_{32}$	-	55, 229, 257, 272	25±2	364±24
2084±1	2084±1	$C_{20}H_{34}O$	1438-62-6	13-epi-manool	238±16	750±49
2266±1	2266±1	$C_{20}H_{32}$	-	55, 133, 120, 272	75±5	462±30

[a] Kovats index (KI), TD-GC-MS2 was used for analysis.

[b] Arithmetic index (AI), TD-GC-MS2 was used for analysis.

[c] Identified or proposed compound formula.

[d] the m/z peaks correspond to either the most abundant peaks or to peaks considered to be characteristic for the specific unknown compound.

[e] Emission rate results obtained at 60±1 °C on the 6th of August, 2019.

[f] Emission rate results obtained at 59±1 °C on the 10th of August, 2019.
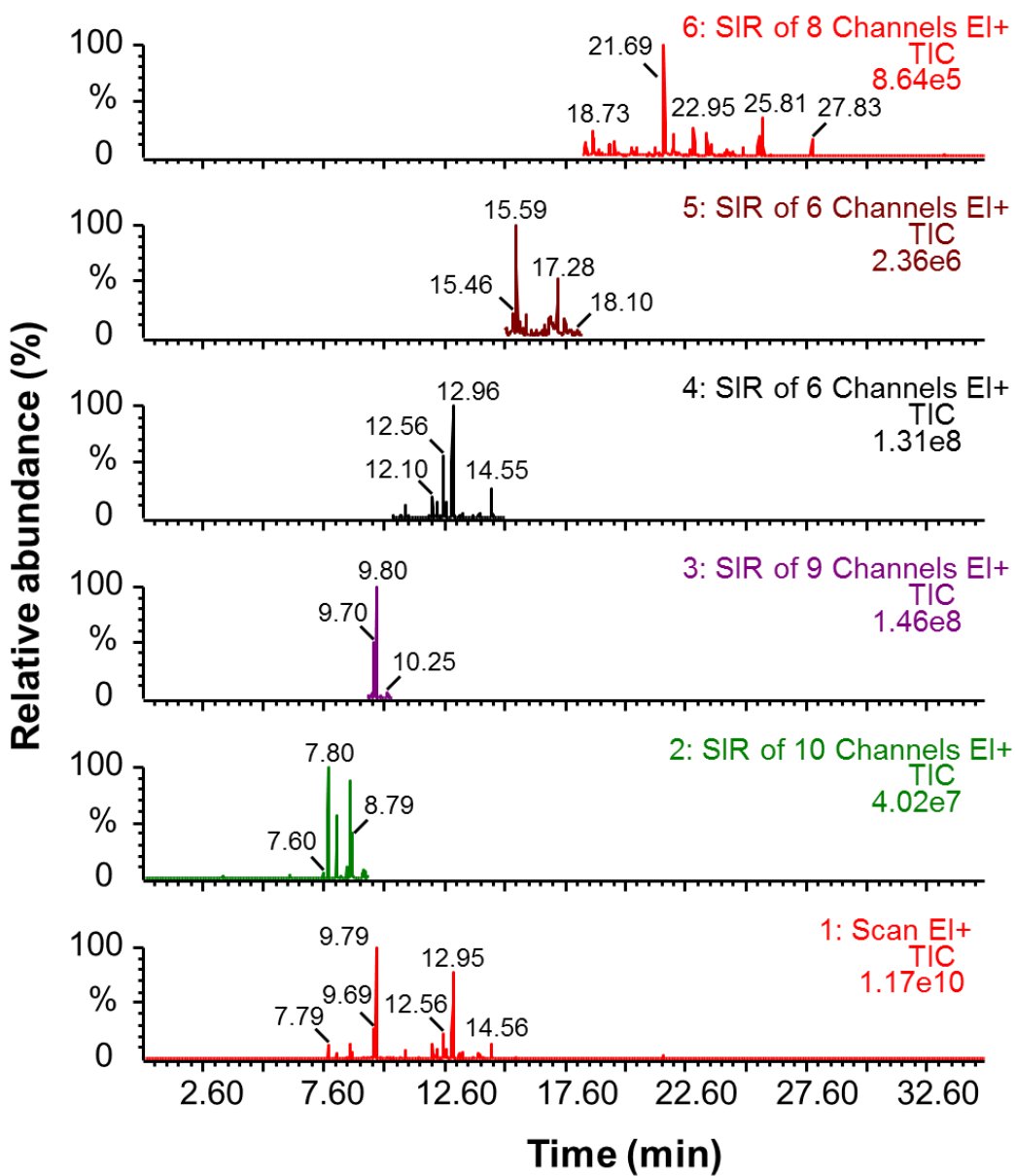
Figure S23. Example of total ion chromatogram (bottom) and selected ion recording (SIR, 2-6) chromatograms from the TD-GC-MS2 analysis of spruce branch enclosure experiment sample on the 10th of August, 2019 (sampling at 59±1 °C for 30 min at flow rate of 100 mL/min).